Am J Transl Res 2021;13(10):11271-11286
www.ajtr.org /ISSN:1943-8141/AJTR0136254

Original Article

MiR-18a-5p acts as a novel serum biomarker for venous malformation and promotes angiogenesis by regulating the thrombospondin-1/P53 signaling axis

Liming Zhang[1*], Deming Wang[1*], Zhenfeng Wang[1], Xiao Li[1], Weiya Xia[2], Yifeng Han[1], Lixin Su[1], Xindong Fan[1]

[1]Department of Interventional Therapy, Shanghai Ninth People's Hospital, Shanghai Jiao Tong University School of Medicine, Shanghai 200011, China; [2]Department of Molecular and Cellular Oncology, The University of Texas MD Anderson Cancer Center, Texas 77030, USA. [*]Equal contributors.

Received June 10, 2021; Accepted August 16, 2021; Epub October 15, 2021; Published October 30, 2021

Abstract: Venous malformation (VM) is a kind of congenital vascular anomaly with high recurrence, and screening for VM lacks an efficient, inexpensive and noninvasive approach now. Serum miRNAs with stable structures are expected to become new postoperative and postablative monitoring biomarkers. Thus, we identified a prognostic serum miR-18a-5p and validated its function in VM. Notably, higher expression level of miR-18a-5p was detected in VM patients than in healthy individuals. We found that miR-18a-5p plays a promotive role in human umbilical vein endothelial cells in vitro. In addition, immunohistochemistry (IHC) results showed a distinct increase of vessels in miR-18a-5p mimics group and a decrease of vessels in inhibitors group compared to the control group in a murine VM model. Furthermore, thrombospondin-1 (TSP1), a potential miR-18a-5p-binding protein, was identified via RNA-seq, luciferase reporter and RNA immunoprecipitation (RIP) assays. Moreover, miR-18a-5p regulated the activation of P53 signaling pathway constituents and consequently led to the regulation of proliferation, migration, invasion and angiogenesis. These results provide a strong theoretical basis for further investigations into pathological mechanism of VM and may provide novel and noninvasive biomarker for VM diagnosis and monitoring.

Keywords: Serum, miR-18a-5p, biomarker, venous malformation, thrombospondin-1, P53

Introduction

Venous malformation (VM) is a commonly encountered vascular malformation with an incidence of approximately 1% of the population [1, 2]. Deficits in venous network development lead to dysfunctional venous channels [3, 4]. These low-flow venous sacs develop at birth and progressively expand along with age; ultimately, these sacs infiltrate and compress normal adjacent tissues [5]. Clinically, symptoms of VM range from small blue localized varicosities to massively swollen lesions [6]. VM may result in not only pain and coagulation abnormalities, but also some potentially life-threatening complications [7] (**Figure 1A**). There are several treatment techniques available, including sclerotherapy, surgery and laser ablation [8], however, there is currently no standard treatment for VM, and the outcomes of some patients are still not satisfactory, especially for those with massive lesions. Thus, efficient evaluation and screening of VM is still a medical challenge.

MicroRNAs (miRNAs) are 18 to 25 nucleotides non-coding RNAs that regulate numerous pathological processes by binding to target mRNA sequences and inhibiting translation [9, 10]. Previous studies showed that miRNAs are relatively stable in serum, which makes it possible to monitor the presence and progression of diseases via miRNA analysis [11-14]. A previous study reported that miR-145 may be involved in the sclerotherapy of VM [15] despite not having a valuable clinical function, so more researches are needed to find promising miRNAs in blood for the evaluation and management of VM. MiR-18a-5p, belonging to the miR-17-92 miRNA cluster, has been reported to participate in brain arteriovenous malformations (BAVMs) [16] and pulmonary arterial

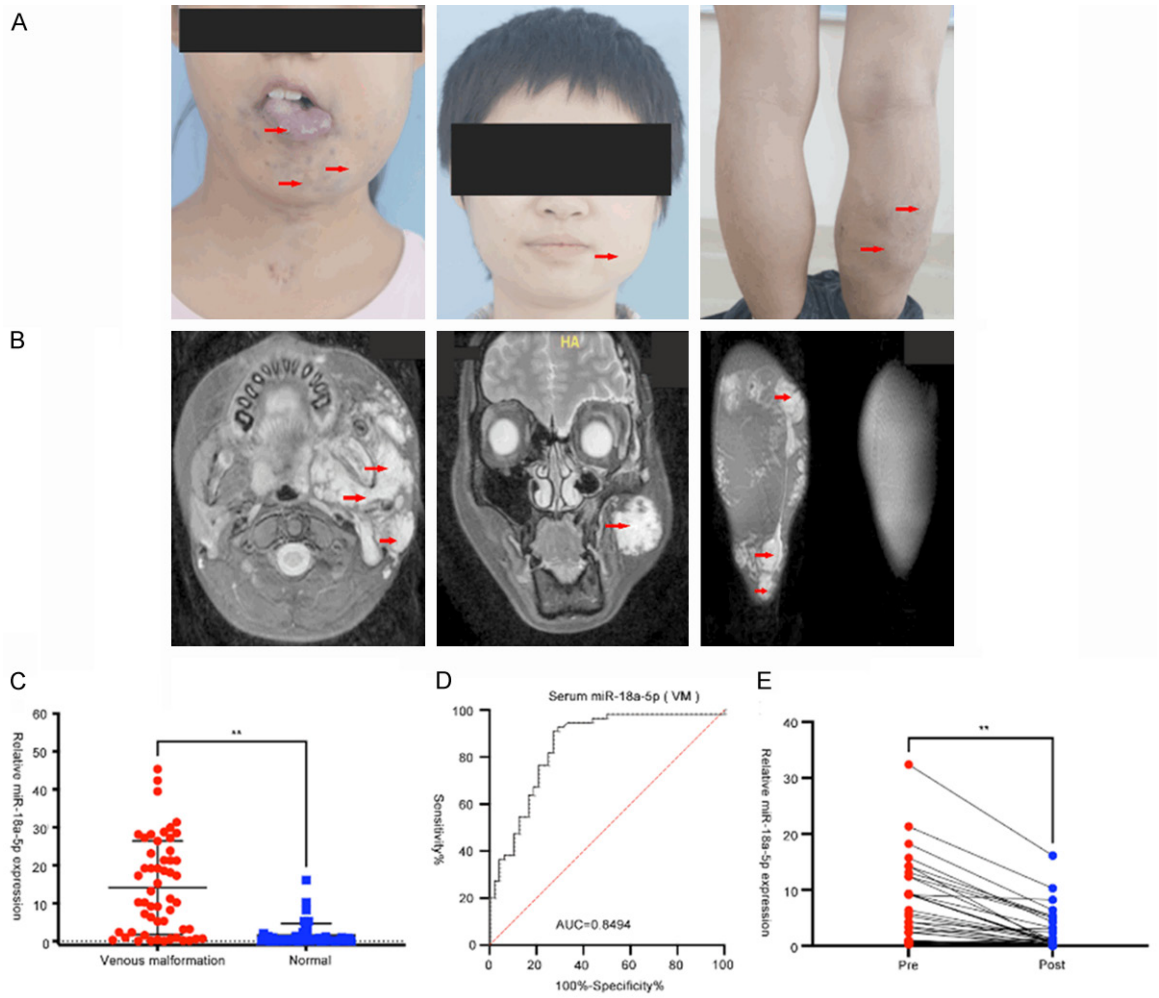

Figure 1. Serum expression of miR-18a-5p in VM patients. A. VM lesions involving the tongue, face and legs, which seriously affected the appearance and function of patients. Red arrows represent the VM lesions. B. The MRI imaging below shows extensive disordered vessels. Red arrows represent the VM lesions. C. A comparison of serum miR-18a-5p levels in VM patients and healthy controls (unpaired t test, $^{**}P<0.05$). D. The diagnostic accuracy of serum miR-18a-5p for discriminating VM patients and healthy controls. E. Comparison of serum miR-18a-5p in paired pre- and post-operative samples (n = 41). $^{**}P<0.05$ (paired t test). Data were obtained from three independent repeated experiments. $^{**}P<0.05$; n.s.: not significant.

hypertension (PAH) [17], indicating that miR-18a-5p may contribute to the process of angiogenesis. Besides, a previous study has reported that miR-18a-5p can function as an effective index of radio-sensitivity in treating lung cancer [18]. Although miR-18a-5p has been characterized regarding its function in many diseases, its role in the pathophysiology of VM has yet to be elucidated.

In this work, we first studied serum samples from venous malformation patients and analyzed the level of angiogenic-related miR-18a-5p, which could potentially act as a serum biomarker for monitoring VM. In addition, we performed some studies to identify the potential target genes of miR-18a-5p and explored the regulatory mechanisms of miR-18a-5p function in venous malformation.

Materials and methods

Clinical samples

No patients received any therapy prior to treatment. We collected 143 serum samples from 102 participants, including 54 patients with VM and 48 healthy controls. The 54 patients were diagnosed with venous malformation by their clinical features and magnetic resonance imaging (MRI). They were recruited at the Ninth People's Hospital between 2019 and 2020

(**Figure 1B**). Blood and serum samples from all participants were collected and stored at -80°C. We obtained informed consent from all participants for publication of identified information/images in an online open-access publication. The performance of the study followed the guidelines of the committee and the Declaration of Helsinki. All experiments were performed in accordance with the relevant guidelines and regulations. Our study was approved by the Ethics Review Committee of the Ninth People's Hospital at the Shanghai Jiao Tong University School of Medicine.

Cell culture and infection

Human umbilical vein endothelial cells (HUVECs) were ordered from ScienCell (USA). The cells underwent mycoplasma testing and short tandem repeat (STR) analyses. Cells were cultured with MEM-α medium (Gibco, USA), including 10% fetal bovine serum (FBS) and 100 mg/ml streptomycin (Gibco, USA) and 1% penicillin). Cells were incubated at 37°C in a humidified atmosphere consisting of 5% CO_2. siTSP1, NC siRNA, TSP1 overexpression (OE) vector, NC OE vector, miR-18a-5p mimics, NC mimics, miR-18a-5p inhibitors, NC inhibitors, miR-18a-5p overexpressing (OE)-lentivirus and miR-18a-5p knockdown (KD)-lentivirus were synthesized by Genome Co. (Shanghai, China). In addition, HUVECs were screened by puromycin after lentivirus infection.

Immunohistochemistry (IHC)

IHC was performed on paraformaldehyde-fixed paraffin-embedded sections with antibodies targeting CD31, P53, bax, bcl-2 (Cell Signaling Technology) and TSP1 (Proteintech Group). Visualization was conducted via the streptavidin-peroxidase conjugation method.

Bioinformatic prediction of miR-18a-5p targets

Common genome-wide targets of miR-18a-5p were explored by using online website starBase (http://starbase.sysu.edu.cn/).

Luciferase reporter assay

We transfected pmirGLO, pmirGLO-NC-wt, pmirGLO-TSP1-wt or pmirGLO-TSP1-mut into miR-18a-5p-overexpressing HUVECs by using Lipofectamine 2000 reagent (Invitrogen, USA). The specific experimental steps were described in our previous published articles [19]. The luciferase activity was detected by Dual-Luciferase System (Promega, USA).

HE staining

We fixed matrigel nodules from animals of different group in 4% paraformaldehyde, and after 24 h, we used a gradient series of alcohol for dehydration. The details of the HE assays were described in our previous article [19]. At last, the sections were sequentially dehydrated with a gradient and fluorescence imaging was used to find the potential changes of blood vessels.

Western blotting (WB)

WB was done as described in our previous article [19]. Antibodies (1:1000) specific for TSP1, bax, P53, bcl-2, and GAPDH were bought from Cell Signaling Technology (Boston, MA, USA). Anti-p-TIE2 antibody was purchased from Affinity Biosciences (Cat# AF2424) (1:1000). All original uncropped gels of Western blot assay were shown in Supplementary Figure 1.

Statistical analysis

Data are expressed as the mean ± SD and comparisons between two groups were performed using an independent sample t-test. Data among multiple groups were compared by one-way analysis of variance (ANOVA). Statistical analyses were performed by SPSS 20.0 (SPSS, Chicago, IL, USA) and plotting and graphing were performed by GraphPad Prism 9.0 (GraphPad Software, San Diego, CA, USA). P value <0.05 was considered as statistically significant.

Supplementary methods

RNA extraction and quantitative real-time polymerase chain reaction, cell proliferation assay, transwell assay, wound healing assay, in vitro tube formation assay, RNA immunoprecipitation and establishment of an animal model of VM are described in Supplementary File 1.

Results

Serum level of miR-18a-5p in VM patients

We first conducted a comprehensive comparative analysis of serum miR-18a-5p level between 54 VM patients and 48 healthy donors. Serum expression of miR-18a-5p was dramatically higher in VM patients than in

Table 1. Clinicopathological features correlated with serum miR-18a-5p expression in VM patients

Characteristics	Number of cases (%)	Expression of serum miR-18a-5p		*P*-value
		High (%)	Low (%)	
Sex				
Male	26 (48.1)	9 (34.6)	17 (65.4)	*0.0293***
Female	28 (51.9)	18 (64.3)	10 (35.7)	
Ages, years				
≤18	27 (50.0)	9 (33.3)	18 (66.7)	*0.0143***
>18	27 (50.0)	18 (66.7)	9 (33.3)	
Max length, cm				
≤2 cm	23 (42.6)	3 (13.0)	20 (87.0)	
>2 cm, ≤4 cm	22 (40.7)	17 (77.3)	5 (22.7)	*0.00005***
>4 cm	9 (16.7)	8 (88.9)	1 (11.1)	
Location				
Lips	11 (20.4)	6 (54.5)	5 (45.5)	
Cheek	6 (11.1)	3 (50.0)	3 (50.0)	
Orbital	3 (5.6)	2 (66.7)	1 (33.3)	
Tongue	22 (40.7)	10 (45.5)	12 (54.5)	*0.7675*
Limb	4 (7.4)	2 (50.0)	2 (50.0)	
Body	2 (3.7)	1 (50.0)	1 (50.0)	
Other	6 (11.1)	3 (50.0)	3 (50.0)	

Abbreviations: VM, venous malformation; Max length, maximum length of VM according to the MRI results; **P<0.05.

healthy group (**Figure 1C**). Then, we performed ROC analyses to evaluate the accuracy of miR-18a-5p for predicting VM. We found that serum miR-18a-5p can well discriminate patients with VM and healthy group, and the AUC value is 0.8494 (sensitivity = 90.91%, specificity = 72.92%) (**Figure 1D**). In addition, we obtained pre- and post-operative serum with 41 successfully managed VM patients, and found that serum miR-18a-5p expressions of these patients were significantly downregulated after treatment (**Figure 1E**). These results indicated that miR-18a-5p has a potential to be a novel serum biomarker for VM screening. In addition, we evaluated the correlations between patients' clinical characteristics and miR-18a-5p expression, all data are summarized in **Table 1**. Sex, age and maximum length of VMs were highly associated with serum level of miR-18a-5p. Female, age >18 and bigger VMs corresponded to higher serum miR-18a-5p level.

MiR-18a-5p promoted cell proliferation, invasion, migration and angiogenesis of HUVECs in vitro and in vivo

To explore biological function of miR-18a-5p in VM, mimics and inhibitors were separately transfected into HUVECs, and the transfection efficiency was validated via qRT-PCR (**Figure 2A**). We then applied CCK-8 to check the effect of miR-18a-5p on HUVEC proliferation and observed that increased miR-18a-5p contributed to the proliferation of HUVEC, while decreased miR-18a-5p attenuated HUVEC proliferation (**Figure 2B**). Then wound healing and transwell assays were used to examine cell invasion and migration. As shown in **Figure 2C**, **2E** and **2F**, miR-18a-5p mimics enhanced HUVEC invasion and migration, but these activities were suppressed by miR-18a-5p inhibitors. Besides, tube formation assay (an in vitro measure of angiogenesis) showed that the tube-forming ability of HUVECs was enhanced with miR-18a-5p mimics and suppressed with miR-18a-5p inhibitors (**Figure 2D**, **2F**).

Venous malformation mouse model was constructed with previous study results [20] (**Figure 2G**). First, we constructed the lentivirus owning TIE2-WT-GFP or TIE2-L914F mutant-GFP, then we infected HUVECs with lentivirus. After infecting, we used WB to check the transfection efficiency (**Figure 2H**). The results showed that the level of phosphorylated TIE2 in HUVECs infected with TIE2-L914F mutant was higher than that of TIE2-WT group. Then, 5×10^6 HUVECs infecting lentivirus were inoculated into one side of mice in an equal volume of Matrigel subcutaneously, and the masses were resected 2 weeks after inoculation (**Figure 2I**). The TIE2-L914F mutation group showed masses with more vessel-like formations, and HE staining revealed that the HUVECs infecting TIE2-L914F mutation could cause more vessels (**Figure 2J**).

To validate whether miR-18a-5p has an effect on angiogenesis in vivo, TIE2-L914F mutant HUVECs were transfected with miR-18a-5p inhibitors, mimics or vehicle for 72 h. Three groups of cells with different treatments were seeded into mice as previously described

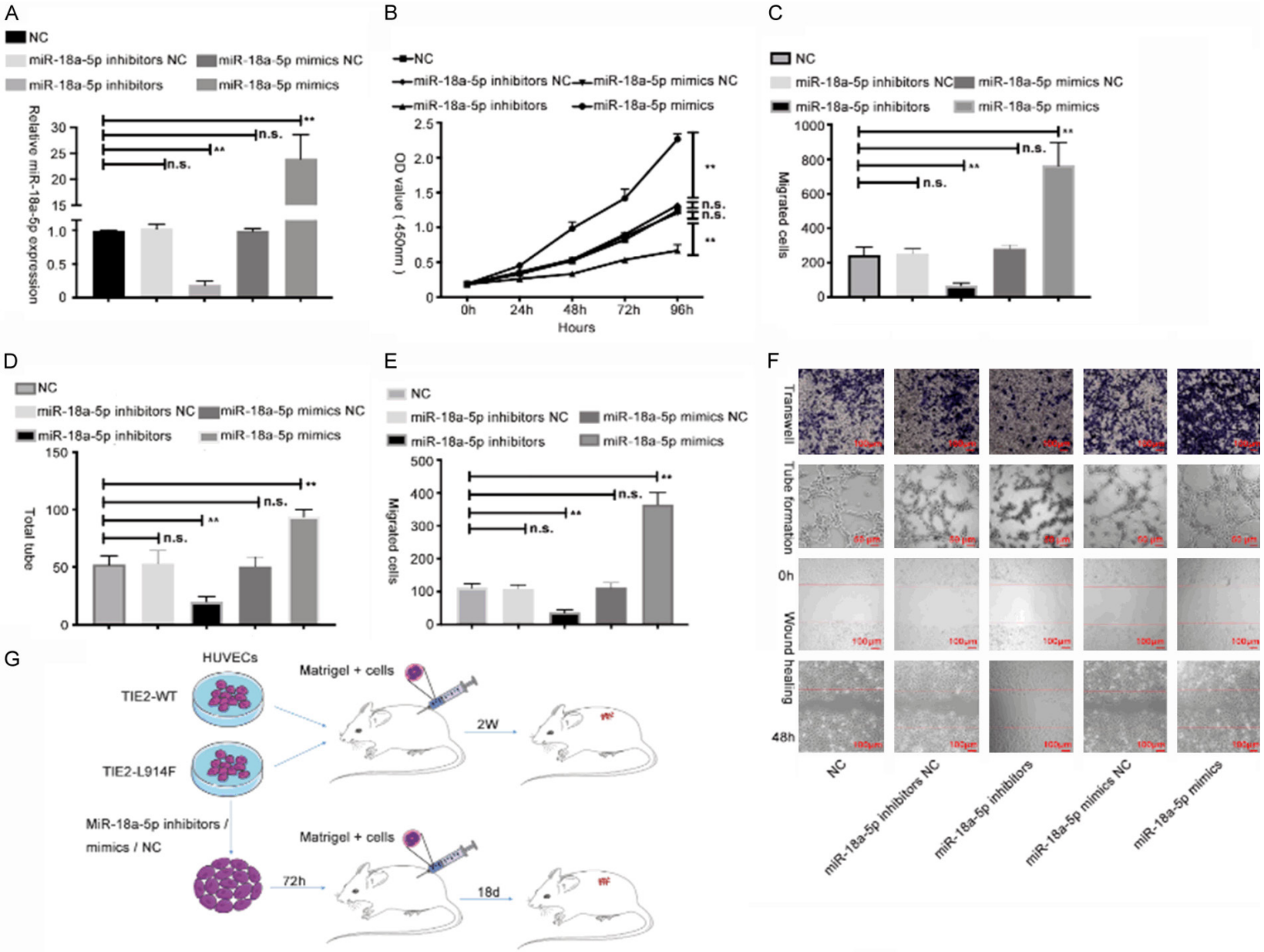
A
NC
miR-18a-5p inhibitors NC
miR-18a-5p mimics NC
miR-18a-5p inhibitors
miR-18a-5p mimics
Relative miR-18a-5p expression
n.s.
B
OD value (450nm)
Hours
0h
24h
48h
72h
96h
C
Migrated cells
D
Total tube
E
Migrated cells
F
Transwell
Tube formation
0h
Wound healing
48h
NC
miR-18a-5p inhibitors NC
miR-18a-5p inhibitors
miR-18a-5p mimics NC
miR-18a-5p mimics
G
HUVECs
TIE2-WT
TIE2-L914F
MiR-18a-5p inhibitors / mimics / NC
Matrigel + cells
2W
72h
18d

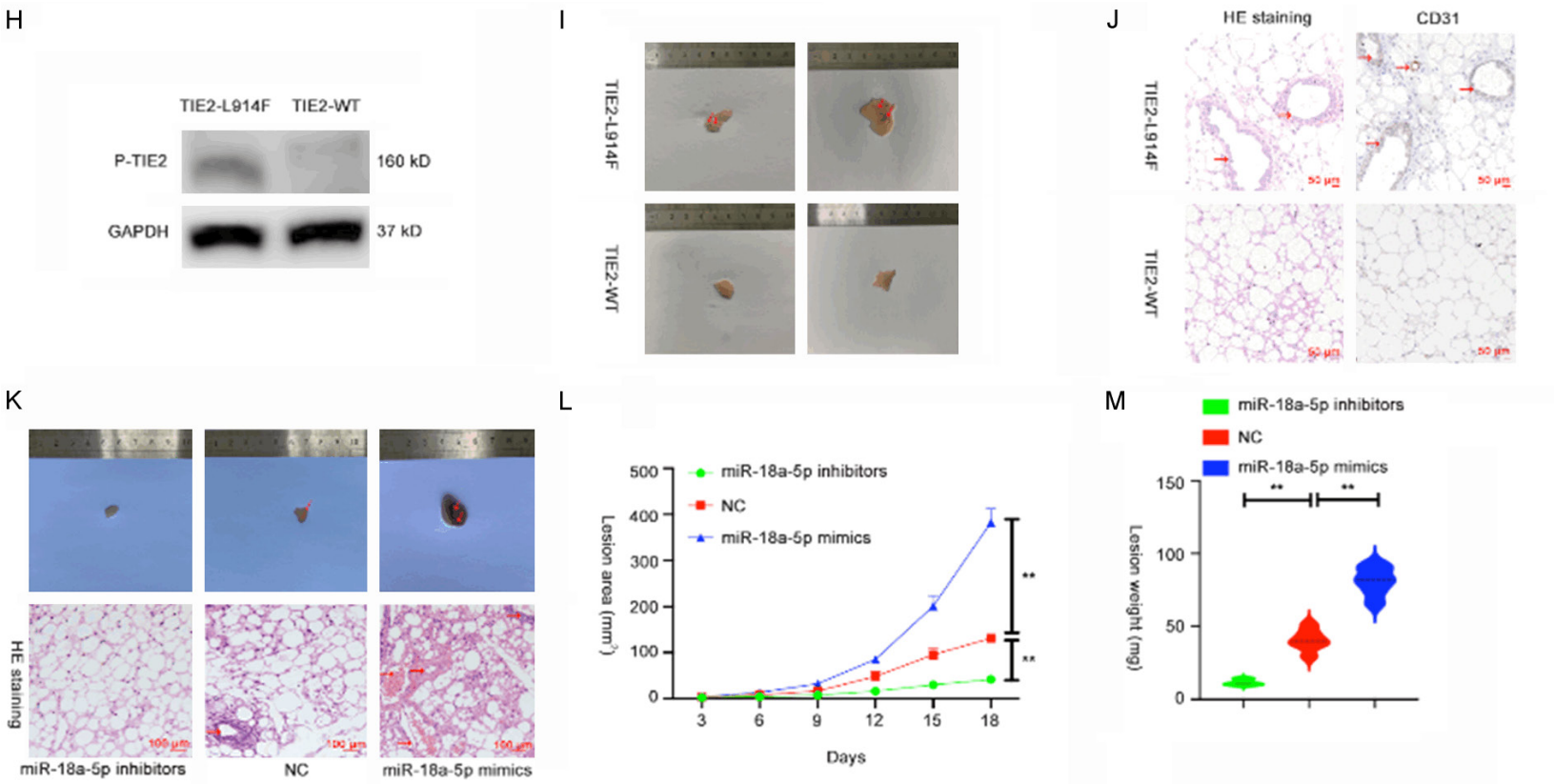

Figure 2. MiR-18a-5p promoted cell proliferation, invasion, migration and angiogenesis of HUVECs in vitro and in vivo. (A) MiR-18a-5p expression was measured via qRT-PCR in HUVECs transfected with plasmids for 48 h. (B) Cell viability was measured by CCK-8 assay in HUVECs transfected with miR-18a-5p inhibitors, miR-18a-5p mimics or corresponding NCs. (C-F) Results of transwell (C, up F), tube formation (D, middle F), and wound healing assays (E, down F) in HUVECs transfected with miR-18a-5p inhibitors, miR-18a-5p mimics or corresponding NCs. (G) Schematic diagram: establishment and treatment of the VM mouse model. (H) The phosphorylated TIE-2 level was detected by Western blot assay. (I) The lesions were harvested 2 weeks after inoculation. (J) H&E and CD31 staining of the lesions. (K) Lesions and H&E staining at 18 days after inoculation of VM model mice subjected to different treatments. (L) Growth curve of the lesion area shows the speed of VM mass growth. (M) The weight of masses excised from mice in the ectopic expression and vector groups were measured and analyzed. The relative expression fold changes in mRNA expression were calculated by the $2^{-\Delta\Delta Ct}$ method. Data were obtained from three independent repeated experiments. $^{**}P<0.05$; n.s.: not significant.

(**Figure 2K**). We measured the masses every 3 days and harvested them 18 days after treatment. We observed that miR-18a-5p inhibitors group showed the least vessel formation, and the extent of vessel formation was medium in the vehicle group, whereas miR-18a-5p mimics group showed the most vessels by H&E staining (**Figure 2K**). Compared to the vehicle group, the miR-18a-5p inhibitors group presented smaller lesion areas and lower total weight of the masses, while the miR-18a-5p mimics group manifested larger lesions and a larger total weight (**Figure 2L**, **2M**). Thus, we hypothesized that miR-18a-5p plays a promotive role in VM progression in vivo and in vitro.

Identification of miR-18a-5p target genes in HUVECs

To study the regulatory mechanisms of miR-18a-5p in HUVECs, we constructed stable miR-18a-5p-overexpressing (OE) and miR-18a-5p-knockdown (KD) HUVECs by infecting the cells with lentivirus (**Figure 3A**). Then, we used RNA-seq to discriminate the differentially expressed genes between the overexpressing group, control group and knockdown group. We used a Venn diagram to show all differentially expressed genes (**Figure 3B** and Supplementary Figure 2A-D). And in **Figure 3C**, 7 miR-18a-5p-regulated genes with significant fold changes were chosen to be validated in HUVECs. qRT-PCR was conducted to evaluate the level of indicated genes in HUVECs transfected with either lentivirus-miR-18a-5p OE or KD. Results showed that thrombospondin-1 (TSP1) exhibited the largest change compared with the other 6 genes; thus, we chose TSP1 for further study (**Figure 3C**). We then did Western blot to validate the expression of TSP1 in miR-18a-5p OE or KD groups (**Figure 3D**). It is well known that miRNAs mostly bind to the 3' UTR region of target mRNAs [21]. To determine potential binding sites that interact with miR-18a-5p, we used starBase 3.0, an online public resource that identifies target mRNAs of miRNAs, to identify the binding sites. To verify whether the biological functions of miR-18a-5p are dependent on the binding to the 3' UTR of TSP1, we constructed a luciferase reporter vector containing the TSP1 3' UTR with wild-type or mutated miR-18a-5p binding site (**Figure 3E**). And results showed that, luciferase activity of the TSP1 3' UTR wild-type reporter was decreased when HUVECs were transfected with the miR-18a-5p mimics but has no significant difference when transfected with scramble control or when miR-18a-5p mimics were co-transfected with the mutant TSP1 3' UTR reporter (**Figure 3F**).

We further analyzed whether miR-18a-5p form the RISC complex with TSP1 by conducting an RIP assay. In brief, FLAG-tagged AGO_2 (Argonaute 2) was overexpressed in HUVECs. And then endogenously bound RNAs were pulled down and purified, followed by qRT-PCR analysis. We postulated that if miR-18a-5p can bind TSP1 mRNA, miR-18a-5p overexpression could lead to a raise of TSP1 mRNAs with AGO_2 (**Figure 3G**). Lastly, an enrichment of TSP1 mRNA with AGO_2 in cells overexpressing miR-18a-5p was validated (**Figure 3H**). All these data indicated that miR-18a-5p guides AGO_2 proteins to TSP1 mRNA. Thus, we concluded that miR-18a-5p directly regulates TSP1 gene in HUVECs.

TSP1 restored the function of miR-18a-5p in HUVECs

To explore the mechanism of TSP1 in HUVECs, we first transfected TSP1 siRNA and a vector into HUVECs, and then checked their efficiency via qRT-PCR and Western blot assays (**Figure 4A**, **4B**). We then explore the role of TSP1 in HUVECs by performing CCK-8, wound healing, tube formation and transwell assays (**Figure 4C-G** and Supplementary Figures 2B, 3A). All the assay results showed that TSP1 can inhibit proliferation, invasion, angiogenesis and migration in HUVECs. Next, we performed rescue experiments by downregulating TSP1 expression in miR-18a-5p KD HUVECs and upregulating TSP1 expression in miR-18a-5p OE HUVECs. We found that TSP1 can restore the promotive role of miR-18a-5p in HUVECs (**Figure 4H-K** and Supplementary Figure 3C-E). These data further support our hypothesis that miR-18a-5p exerts its function by regulating TSP1 expression in HUVECs.

Verification of the regulatory relationship between miR-18a-5p and the P53 signaling pathway in vitro and in vivo

According to the results of GO function and KEGG pathway enrichment analyses (**Figure 5A** and Supplementary Figure 4A-C), P53 signaling

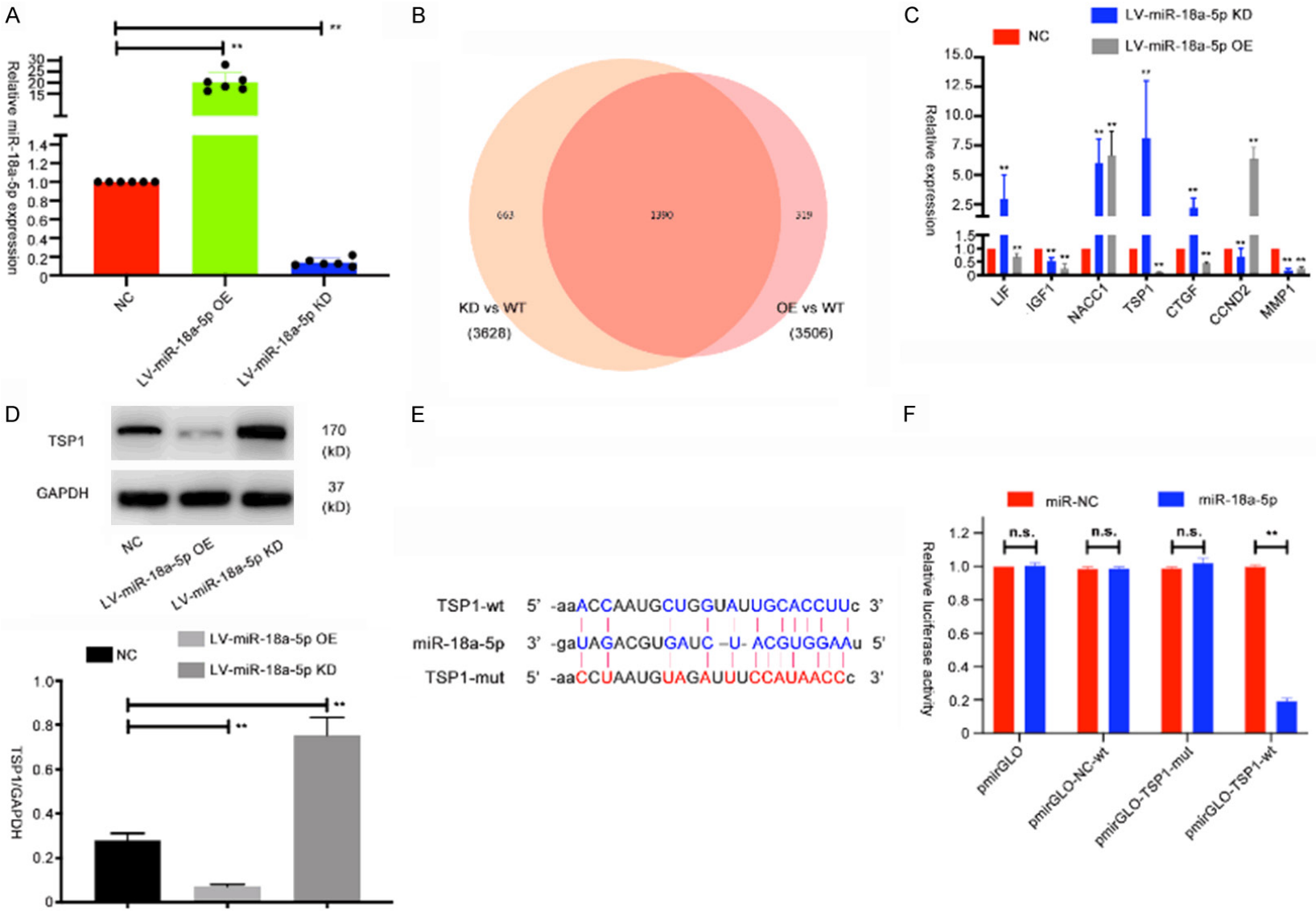
A
Relative miR-18a-5p expression
NC
LV-miR-18a-5p OE
LV-miR-18a-5p KD
B
663
1390
329
KD vs WT
(3628)
OE vs WT
(3506)
C
NC
LV-miR-18a-5p KD
LV-miR-18a-5p OE
Relative expression
LIF
IGF1
NACC1
TSP1
CTGF
CCND2
MMP1
D
TSP1
GAPDH
170
(kD)
37
(kD)
NC
LV-miR-18a-5p OE
LV-miR-18a-5p KD
NC
LV-miR-18a-5p OE
LV-miR-18a-5p KD
TSP1/GAPDH
E
TSP1-wt 5' -aaACCAAUGCUGGUAUUGCACCUUc 3'
miR-18a-5p 3' -gaUAGACGUGAUC -U- ACGUGGAAu 5'
TSP1-mut 5' -aaCCUAAUGUAGAUUUCCAUAACCc 3'
F
miR-NC
miR-18a-5p
Relative luciferase activity
n.s.
n.s.
n.s.
pmirGLO
pmirGLO-NC-wt
pmirGLO-TSP1-mut
pmirGLO-TSP1-wt

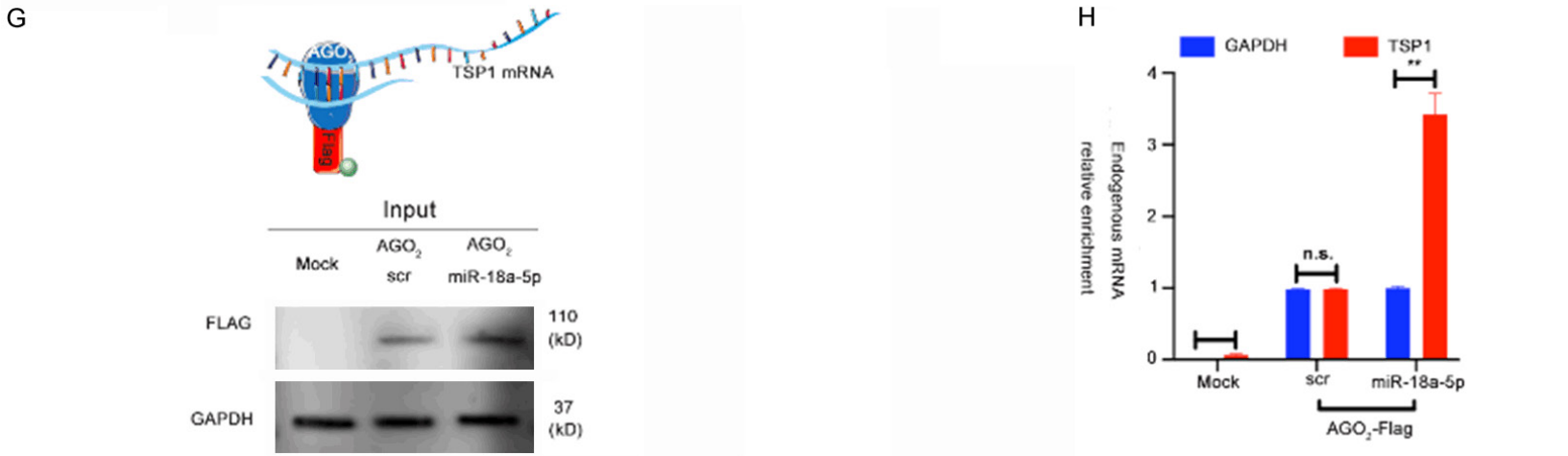

Figure 3. Identification of miR-18a-5p target genes in HUVECs. A. Expression levels of miR-18a-5p in HUVECs transfected with lentivirus either overexpressing miR-18a-5p (OE) or miR-18a-5p knockdown (KD). B. Venn diagram and prediction legends of the target genes regulated by miR-18a-5p in HUVECs. C. Relative expression of putative target genes in HUVECs transfected with NC, miR-18a-5p OE or miR-18a-5p KD. D. Expression levels of TSP1 were measured via Western blot in HUVECs transfected with NC, miR-18a-5p OE or miR-18a-5p KD. E. Potential miR-18a-5p base pairing alignment with TSP1 (blue), as identified by starBase v3.0. A mutation in the putative binding site was also established (red). F. Luciferase activity in HUVECs co-transfected with miR-18a-5p mimics and luciferase reporters containing empty vector, TSP1-wt or TSP1-mutant transcripts. G. Scheme of the RIP assay of AGO_2-FLAG pull-down and RT-qPCR analysis of endogenous mRNA enrichment upon miR-18a-5p overexpression. H. QRT-PCR analysis of endogenous TSP1 mRNA upon immunoprecipitation of AGO_2-FLAG in one representative experiment of three replicates. Data were obtained from three independent repeated experiments. $^{**}P<0.05$; n.s.: not significant.

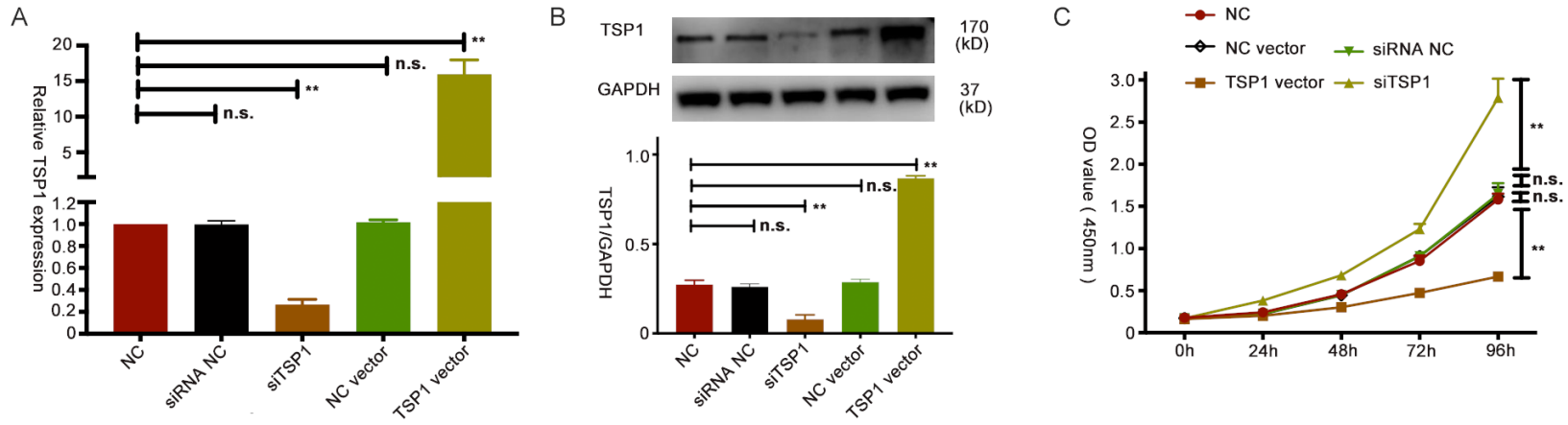

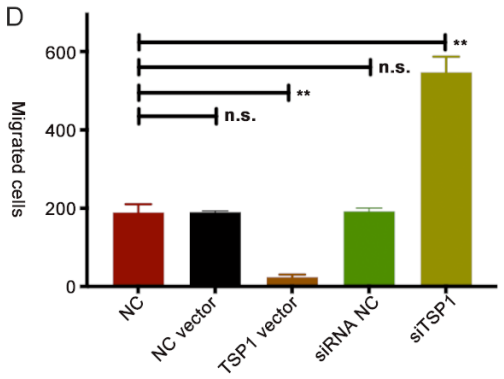
D
Migrated cells
600
400
200
0
**
n.s.
**
n.s.
NC
NC vector
TSP1 vector
siRNA NC
siTSP1

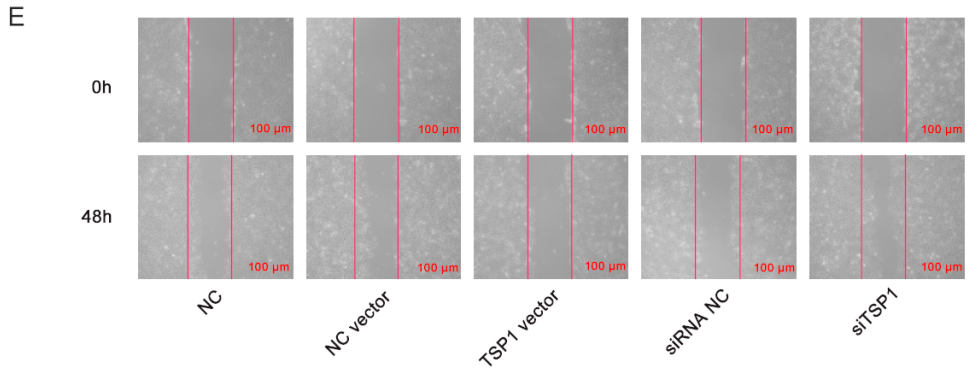
E
0h
48h
100 μm
NC
NC vector
TSP1 vector
siRNA NC
siTSP1

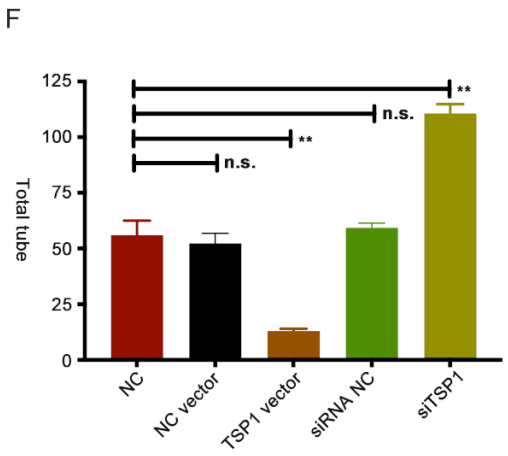
F
Total tube
125
100
75
50
25
0
**
n.s.
**
n.s.
NC
NC vector
TSP1 vector
siRNA NC
siTSP1

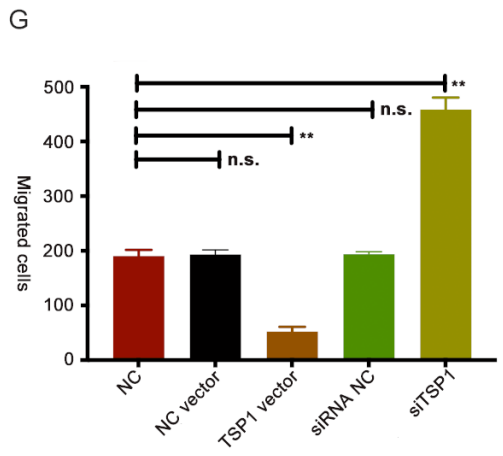
G
Migrated cells
500
400
300
200
100
0
**
n.s.
**
n.s.
NC
NC vector
TSP1 vector
siRNA NC
siTSP1

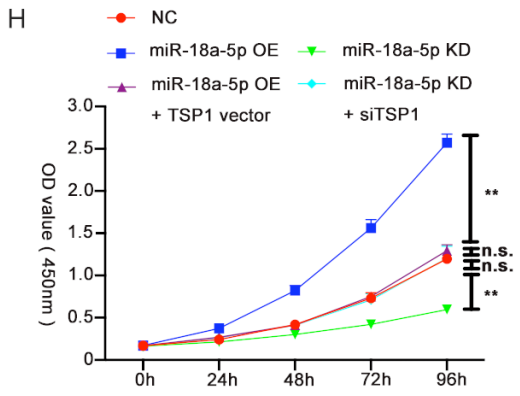
H
NC
miR-18a-5p OE
miR-18a-5p KD
miR-18a-5p OE
+ TSP1 vector
miR-18a-5p KD
+ siTSP1
OD value (450nm)
3.0
2.5
2.0
1.5
1.0
0.5
0
0h
24h
48h
72h
96h
**
n.s.
n.s.
**

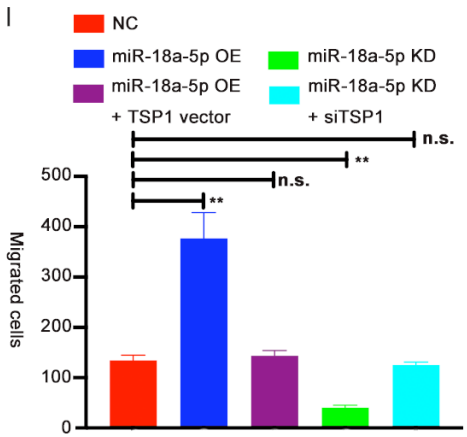
I
NC
miR-18a-5p OE
miR-18a-5p KD
miR-18a-5p OE
+ TSP1 vector
miR-18a-5p KD
+ siTSP1
Migrated cells
500
400
300
200
100
0
n.s.
**
n.s.
**

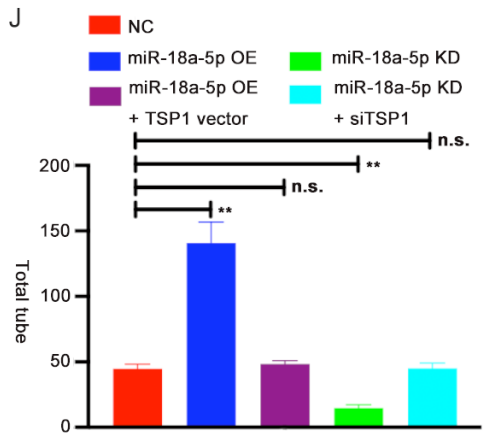
J
NC
miR-18a-5p OE
miR-18a-5p KD
miR-18a-5p OE
+ TSP1 vector
miR-18a-5p KD
+ siTSP1
Total tube
200
150
100
50
0
n.s.
**
n.s.
**

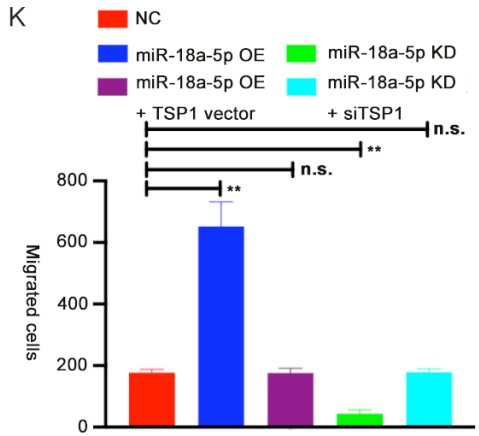
K
NC
miR-18a-5p OE
miR-18a-5p KD
miR-18a-5p OE
+ TSP1 vector
miR-18a-5p KD
+ siTSP1
Migrated cells
800
600
400
200
0
n.s.
**
n.s.
**

Figure 4. TSP1 restored the function of miR-18a-5p in HUVECs. (A, B) Expression of TSP1 in HUVECs transfected with siRNA NC, siTSP1, NC vector and TSP1 vector was examined by qRT-PCR (A) and Western blot (B). (C) The viability of HUVECs after transfection with TSP1 vector or siTSP1 was determined using CCK-8 assay. (D, E) A wound healing assay was performed with HUVECs transfected with TSP1 vector or siTSP1. (F, G) Tube formation (F) and transwell assays (G) were conducted in HUVECs with TSP1 vector or siTSP1. (H-K) Growth, invasion, migration and angiogenesis of HUVECs transfected with NC, miR-18a-5p OE, miR-18a-5p KD, miR-18a-5p OE + TSP1 OE vector or miR-18a-5p KD + siTSP1 were evaluated by CCK-8 (H), wound healing (I), tube formation (J) and transwell assays (K). Data were obtained from three independent repeated experiments. **P<0.05; n.s.: not significant.

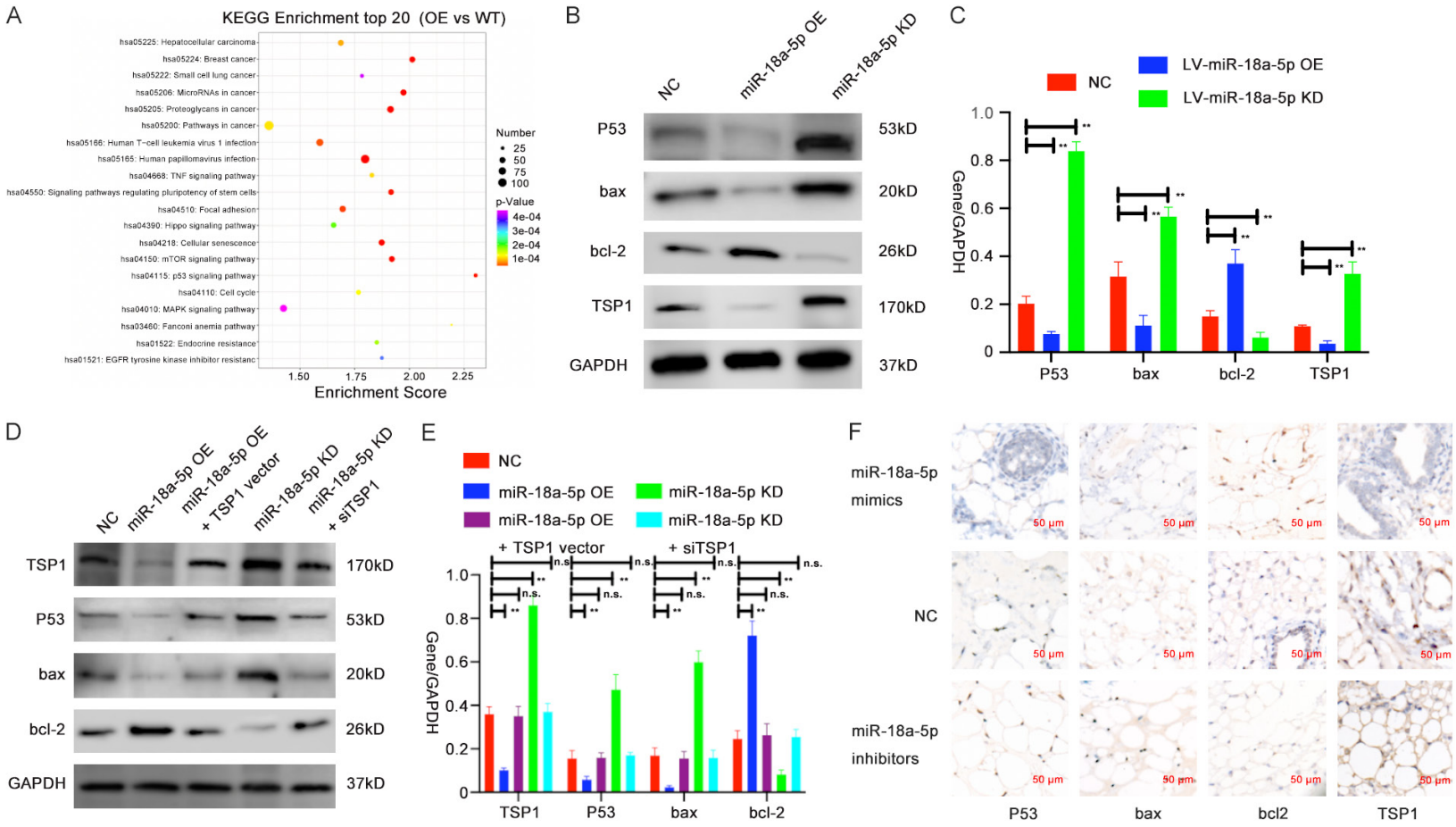

Figure 5. Verification of the regulatory relationship between miR-18a-5p and the P53 signaling pathway in vitro and in vivo. A. KEGG analysis was performed to identify pathway terms enriched in the dysregulated mRNAs in HUVECS with miR-18a-5p OE vs WT. B, C. Western blot analysis of P53 signaling-related protein levels in lysates from HUVECs transfected with NC, miR-18a-5p OE or miR-18a-5p KD. D, E. Expressions of P53 signaling-related protein in NC-, miR-18a-5p OE-, miR-18a-5p KD-, miR-18a-5p OE + TSP1 OE vector, or miR-18a-5p KD + siTSP1-transfected HUVECs were evaluated via Western blotting. F. Relative expression of TSP1 and P53 signaling-related molecules was shown by immunohistochemistry in each group of VM mice model. Data were obtained from three independent repeated experiments. **P<0.05; n.s.: not significant.

pathway showed the highest enrichment score among all the affected pathways after miR-18a-5p levels changed (**Figure 5A** and Supplementary Figure 4A). Therefore, we postulated that miR-18a-5p and its target gene TSP1 may predominantly function through the P53 signaling pathway. Then, we assessed the protein expression of genes related to the P53 signaling pathway (P53, bax, bcl-2) after altering the expression of miR-18a-5p in HUVECs via Western blot assay (**Figure 5B**, **5C**). We found that the expressions of P53, bax, and TSP-1were decreased while that of bcl-2 was increased in miR-18a-5p OE HUVECs; in contrast, the opposite results were observed in miR-18a-5p KD HUVECs.

To explore whether the target gene TSP1 participates in the regulation of miR-18a-5p to P53 signaling pathway, we made the same rescue experiments as for previous groups, extracted their protein and assessed these genes' expression via Western blot assay. We saw that expression of these P53 signaling pathway-related genes did show restored phenomenon when we transfected miR-18a-5p OE HUVECs with TSP1 vector or transfected miR-18a-5p KD HUVECs with siTSP1. Expression of P53, bax and bcl-2 all returned back to the original level in miR-18a-5p OE + TSP1 vector group and miR-18a-5p KD + siTSP1 group compared with the control group. (**Figure 5D**, **5E**).

To validate previous results in vivo, we conducted an IHC assay of the cell-containing Matrigel nodules, and we analyzed the expression of TSP1, P53, bax, bcl-2 in miR-18a-5p mimics, miR-18a-5p inhibitors and control groups. We found that miR-18a-5p mimics group showed higher expression of bcl-2 and lower expression of P53, bax and TSP1, and the miR-18a-5p inhibitors group had lower expression of bcl-2 and higher expression of P53, bax and TSP1 compared with the control group (**Figure 5F**). Thus, we draw a conclusion that miR-18a-5p can promote VM progression by regulating the TSP1/P53 signaling pathway.

Discussion

It was reported that human serum containing miRNAs or cytokines can play important roles in various devastating diseases and infections [22-24]. There has been increasing interest in recent years in the use of human serum components as biomarkers or therapeutic targets [25, 26], particularly in the field of hematopathy. Numerous studies on the role of human serum composition in blood diseases or cancer progression have been published [27-29]. During the developmental process of human diseases, the serum composition varies profoundly. These variations include changes in the quantities and types of various miRNAs, suggesting a potential for human serum to be used for identification, monitoring and treatment of diseases [30, 31]. In our investigation, we measured the expression of serum miR-18a-5p derived from VM patients and healthy donors by quantitative real-time PCR. Our results showed that VM patients had a significantly higher serum miR-18a-5p than the healthy donors, and its expression returned to a relatively normal level when the patients' diseases were successfully controlled. All these results validate that miR-18a-5p could serve as a predictive or monitoring serum biomarker of VM.

According to the most recent studies about the function and regulation of miRNAs in other diseases, lncRNAs and circRNAs can function as competing endogenous RNAs (ceRNAs) by sponging corresponding miRNAs in various psychological and pathological processes. Lots of dysregulated ceRNAs networks have been reported and explored. Thus, another study about the differentially expressed serum exosomal circRNAs and lncRNAs has also been conducted by our team to find the possible molecular mechanism by which miR-18a-5p is up-regulated in VM patients.

Previous studies revealed that miR-18a-5p can participate in many processes of cancers [32, 33]. In addition, miR-18a-5p has also been verified to play a vital role in vascular endothelial cell proliferation, migration, invasion, and angiogenesis [34, 35]. However, the effect of miR-18a-5p on VM is still poorly understood. Our results validated that miR-18a-5p levels were higher in the serum of VM patients than healthy group. Studies showed that miR-18a-5p overexpression significantly enhanced the proliferation, migration, invasion and angiogenesis of HUVECs in vitro. Besides, downregulation of miR-18a-5p gave rise to contrary results. Previous studies have shown that miRNAs can exert their functions by affecting the expres-

sion of their target mRNAs [36]. Thus, to check the predictive binding and explore the potential target genes of miR-18a-5p in HUVECs, mRNA levels in miR-18a-5p knockdown and miR-18a-5p overexpression as well as in control groups were further measured by RNA-seq. Then seven genes showing the largest changes (TSP1, IGF1, CTGF, LIF, CCND2, NACC1 and MMP1) were chosen for further validation, with the TSP1 gene showing the strongest negative correlation with miR-18a-5p as checked by qRT-PCR and Western blot.

Thrombospondins (TSPs) participate in lots of physical and pathological processes, such as cell differentiation, proliferation, vascular hemeostasis and wound healing [37]. Thrombospondin-1 (TSP-1) is one of the thrombospondin family [38], and TSP-1 is mostly synthesized and secreted by platelets and endothelial cells [39]. Numerous studies have reported that TSP1 shows a wide range of biological effects, such as inhibiting angiogenesis, antitumor activity and so on [40]. Taken together, TSP1 might play an important role in the regulation of biological processes. According to our study, the level of TSP1 was directly regulated by miR-18a-5p as indicated by the results of dual-luciferase reporter and RIP assays. Besides, when miR-18a-5p expression changed in HUVECs, ectopic TSP1 expression rescued the promotive role of miR-18a-5p in HUVECs via rescue assays, indicating a latent role of TSP1 in miR-18a-5p regulatory axis in VM.

To explore the detailed mechanism of miR-18a-5p in HUVECs, we performed an RNA-seq assay. By performing KEGG analysis, we saw that P53 signaling pathway was the most important pathway regulated by miR-18a-5p. Previous studies showed that P53 can regulate gene transcription, leading to cell death, DNA injures and changes in angiogenesis [41-45]. More importantly, TSP-1 had been reported to participate in the P53 signaling in several diseases [46-48]. Thus, we decided to validate whether miR-18a-5p function by regulating the P53 signaling pathway to some degree. Remarkably, Western blot analysis of protein level showed that, overexpression of miR-18a-5p downregulated the expression of P53, bax, TSP1 and increased the expression of bcl-2 in HUVECs. By contrast, downregulating miR-18a-5p in HUVECs had the opposite effect on the expression pattern of these genes. Thus, we confirmed that miR-18a-5p can regulate TSP1 expression and further played a significant role in the P53 signaling pathway. Considering the P53 signaling pathway constituents, we also conducted the flow cytometry assay to verify the apoptosis rate of different miR-18a-5p changed groups, but we found that, there was no significant statistical difference between the three groups. Thus we postulated that, TSP1 had the angio-inhibitory signaling downstream of miR-18a-5p that might override other pro-apoptotic signaling. Besides, considering there were also lots of genes regulated by the miR-18a-5p, it may be possible that some molecules among these genes counteracted the apoptotic influence of P53 signaling pathway constituents.

Finally, to verify the function of miR-18a-5p in the vessel formation process in vivo, we established a VM mouse model, and the results suggested that compared to the control, miR-18a-5p inhibitors led to less vessel formation whereas miR-18a-5p mimics caused more vessel formation. We also found that the expression trends of TSP1 and P53 signaling-related proteins were also consistent with the in vitro expression levels in HUVECs by IHC.

To our best knowledge, our study is the first report describing the clinical significance of serum miR-18a-5p in VM. Our results suggest that miR-18a-5p can promote VM progression by suppressing TSP1 and further regulating the P53 signaling pathway (**Figure 6**). Therefore, serum miR-18a-5p might be a promising therapeutic target and serum biomarker for VM.

Acknowledgements

The authors would like to thank Prof. Wayne F. Yakes for teaching the technique of ethanol embolization and supporting clinical work during these years. We thank all the doctors and nurses in our apartment and the work was done with their kind help. This work was supported by National Natural Science Foundation of China (Grant No.81871458) and Clinical Research Program of Ninth People's Hospital, Shanghai Jiaotong University, School of Medicine (Grant No. JYLJ201911 and No. JYLJ201801).

Disclosure of conflict of interest

None.

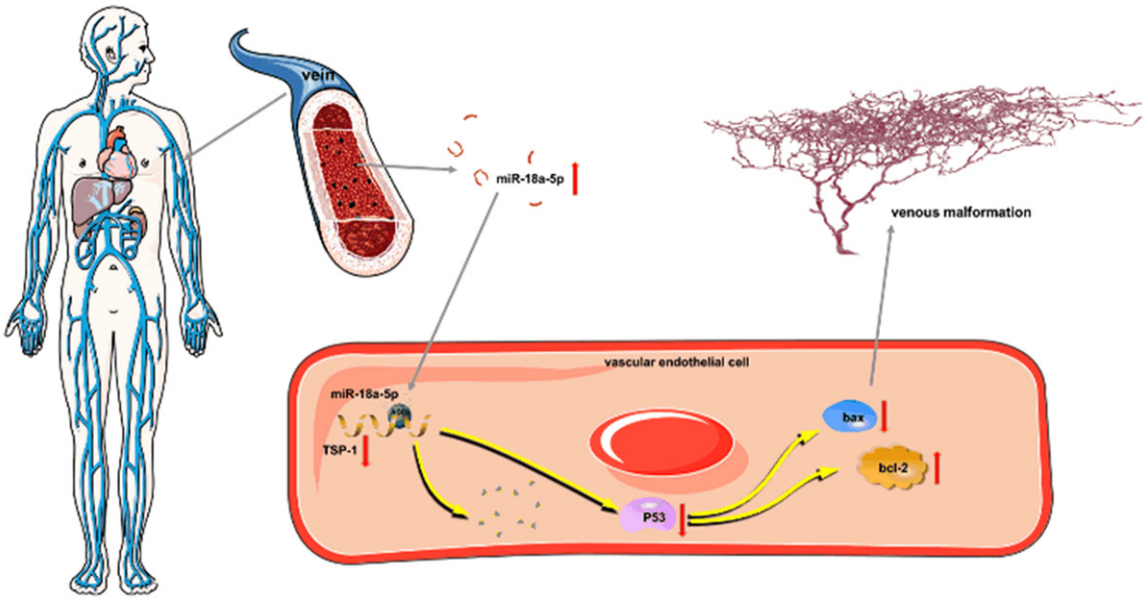

Figure 6. Hypothetical model describing the function of miR-18a-5p in VM. High expression of serum miR-18a-5p downregulates the expression level of TSP-1 in vascular endothelial cells, which participates in the P53 signaling pathway, resulting in VM progression.

Address correspondence to: Xindong Fan and Lixin Su, Department of Interventional Therapy, Shanghai Ninth People's Hospital, Shanghai Jiao Tong University School of Medicine, No. 639 Zhizaoju Road, Shanghai 200011, China. Tel: +86-021-23271699; E-mail: fanxd1964@163.com (XDF); sulixin1975@126.com (LXS)

References

[1] Han YY, Sun LM and Yuan SM. Localized intravascular coagulation in venous malformations: a system review. Phlebology 2021; 36: 38-42.

[2] Olivieri B, White CL, Restrepo R, McKeon B, Karakas SP and Lee EY. Low-flow vascular malformation pitfalls: from clinical examination to practical imaging evaluation--part 2, venous malformation mimickers. AJR Am J Roentgenol 2016; 206: 952-962.

[3] Wassef M, Blei F, Adams D, Alomari A, Baselga E, Berenstein A, Burrows P, Frieden IJ, Garzon MC, Lopez-Gutierrez JC, Lord DJ, Mitchel S, Powell J, Prendiville J, Vikkula M, Board I and Scientific C. Vascular anomalies classification: recommendations from the international society for the study of vascular anomalies. Pediatrics 2015; 136: e203-214.

[4] Limaye N, Wouters V, Uebelhoer M, Tuominen M, Wirkkala R, Mulliken JB, Eklund L, Boon LM and Vikkula M. Somatic mutations in angiopoietin receptor gene TEK cause solitary and multiple sporadic venous malformations. Nat Genet 2009; 41: 118-124.

[5] Dasgupta R and Patel M. Venous malformations. Semin Pediatr Surg 2014; 23: 198-202.

[6] Cheng AC, Li EY, Chan TC, Wong AC, Chan PC, Poon WW, Fung DH and Yuen HK. Hybrid procedure for orbital venous malformation in the endovascular operation room. Eye (Lond) 2015; 29: 1069-1075.

[7] Dompmartin A, Acher A, Thibon P, Tourbach S, Hermans C, Deneys V, Pocock B, Lequerrec A, Labbe D, Barrellier MT, Vanwijck R, Vikkula M and Boon LM. Association of localized intravascular coagulopathy with venous malformations. Arch Dermatol 2008; 144: 873-877.

[8] Seront E, Vikkula M and Boon LM. Venous malformations of the head and neck. Otolaryngol Clin North Am 2018; 51: 173-184.

[9] Goodall GJ and Wickramasinghe VO. RNA in cancer. Nat Rev Cancer 2021; 21: 22-36.

[10] Zhang MW, Shen YJ, Shi J and Yu JG. MiR-223-3p in cardiovascular diseases: a biomarker and potential therapeutic target. Front Cardiovasc Med 2020; 7: 610561.

[11] Mens MMJ, Heshmatollah A, Fani L, Ikram MA, Ikram MK and Ghanbari M. Circulatory MicroRNAs as potential biomarkers for stroke risk: the rotterdam study. Stroke 2021; 52: 945-953.

[12] Komoll RM, Hu Q, Olarewaju O, von Dohlen L, Yuan Q, Xie Y, Tsay HC, Daon J, Qin R, Manns MP, Sharma AD, Goga A, Ott M and Balakrishnan A. MicroRNA-342-3p is a potent tumour suppressor in hepatocellular carcinoma. J Hepatol 2021; 74: 122-134.

[13] Lin XJ, Chong Y, Guo ZW, Xie C, Yang XJ, Zhang Q, Li SP, Xiong Y, Yuan Y, Min J, Jia WH, Jie Y,

Chen MS, Chen MX, Fang JH, Zeng C, Zhang Y, Guo RP, Wu Y, Lin G, Zheng L and Zhuang SM. A serum microRNA classifier for early detection of hepatocellular carcinoma: a multicentre, retrospective, longitudinal biomarker identification study with a nested case-control study. Lancet Oncol 2015; 16: 804-815.

[14] Schultz NA, Dehlendorff C, Jensen BV, Bjerregaard JK, Nielsen KR, Bojesen SE, Calatayud D, Nielsen SE, Yilmaz M, Hollander NH, Andersen KK and Johansen JS. MicroRNA biomarkers in whole blood for detection of pancreatic cancer. JAMA 2014; 311: 392-404.

[15] Xia HF, Ren JG, Zhu JY, Yu ZL, Zhang W, Sun YF, Zhao YF and Chen G. Downregulation of miR-145 in venous malformations: Its association with disorganized vessels and sclerotherapy. Eur J Pharm Sci 2017; 100: 126-131.

[16] Marin-Ramos NI, Thein TZ, Ghaghada KB, Chen TC, Giannotta SL and Hofman FM. miR-18a inhibits BMP4 and HIF-1alpha normalizing brain arteriovenous malformations. Circ Res 2020; 127: e210-e231.

[17] Miao R, Liu W, Qi C, Song Y, Zhang Y, Fu Y, Liu W, Lang Y, Zhang Y and Zhang Z. MiR-18a-5p contributes to enhanced proliferation and migration of PASMCs via targeting Notch2 in pulmonary arterial hypertension. Life Sci 2020; 257: 117919.

[18] Chen X, Wu L, Li D, Xu Y, Zhang L, Niu K, Kong R, Gu J, Xu Z, Chen Z and Sun J. Radiosensitizing effects of miR-18a-5p on lung cancer stem-like cells via downregulating both ATM and HIF-1alpha. Cancer Med 2018; 7: 3834-3847.

[19] Zhang LM, Su LX, Hu JZ, Wang M, Ju HY, Li X, Han YF, Xia WY, Guo W, Ren GX and Fan XD. Epigenetic regulation of VENTXP1 suppresses tumor proliferation via miR-205-5p/ANKRD2/NF-κB signaling in head and neck squamous cell carcinoma. Cell Death Dis 2020; 11: 838.

[20] Boscolo E, Limaye N, Huang L, Kang KT, Soblet J, Uebelhoer M, Mendola A, Natynki M, Seront E, Dupont S, Hammer J, Legrand C, Brugnara C, Eklund L, Vikkula M, Bischoff J and Boon LM. Rapamycin improves TIE2-mutated venous malformation in murine model and human subjects. J Clin Invest 2015; 125: 3491-3504.

[21] Bartel DP. Metazoan MicroRNAs. Cell 2018; 173: 20-51.

[22] Doxakis E. Cell-free microRNAs in Parkinson's disease: potential biomarkers that provide new insights into disease pathogenesis. Ageing Res Rev 2020; 58: 101023.

[23] Kiuchi J, Komatsu S, Imamura T, Nishibeppu K, Shoda K, Arita T, Kosuga T, Konishi H, Shiozaki A, Okamoto K, Fujiwara H, Ichikawa D and Otsuji E. Low levels of tumour suppressor miR-655 in plasma contribute to lymphatic progression and poor outcomes in oesophageal squamous cell carcinoma. Mol Cancer 2019; 18: 2.

[24] Mori MA, Ludwig RG, Garcia-Martin R, Brandao BB and Kahn CR. Extracellular miRNAs: from biomarkers to mediators of physiology and disease. Cell Metab 2019; 30: 656-673.

[25] Willeit P, Skroblin P, Kiechl S, Fernandez-Hernando C and Mayr M. Liver microRNAs: potential mediators and biomarkers for metabolic and cardiovascular disease? Eur Heart J 2016; 37: 3260-3266.

[26] Huang X, Zhu X, Yu Y, Zhu W, Jin L, Zhang X, Li S, Zou P, Xie C and Cui R. Dissecting miRNA signature in colorectal cancer progression and metastasis. Cancer Lett 2021; 501: 66-82.

[27] Garg A, Seeliger B, Derda AA, Xiao K, Gietz A, Scherf K, Sonnenschein K, Pink I, Hoeper MM, Welte T, Bauersachs J, David S, Bar C and Thum T. Circulating cardiovascular microRNAs in critically ill COVID-19 patients short title: microRNA signatures in COVID-19. Eur J Heart Fail 2021; 23: 468-475.

[28] Liebetrau C, Mollmann H, Dorr O, Szardien S, Troidl C, Willmer M, Voss S, Gaede L, Rixe J, Rolf A, Hamm C and Nef H. Release kinetics of circulating muscle-enriched microRNAs in patients undergoing transcoronary ablation of septal hypertrophy. J Am Coll Cardiol 2013; 62: 992-998.

[29] Karakas M, Schulte C, Appelbaum S, Ojeda F, Lackner KJ, Munzel T, Schnabel RB, Blankenberg S and Zeller T. Circulating microRNAs strongly predict cardiovascular death in patients with coronary artery disease-results from the large AtheroGene study. Eur Heart J 2017; 38: 516-523.

[30] Chiacchiarini M, Trocchianesi S, Besharat ZM, Po A and Ferretti E. Role of tissue and circulating microRNAs and DNA as biomarkers in medullary thyroid cancer. Pharmacol Ther 2020; 219: 107708.

[31] Moccia M, Caratelli V, Cinti S, Pede B, Avitabile C, Saviano M, Imbriani AL, Moscone D and Arduini F. Paper-based electrochemical peptide nucleic acid (PNA) biosensor for detection of miRNA-492: a pancreatic ductal adenocarcinoma biomarker. Biosens Bioelectron 2020; 165: 112371.

[32] Zhao W, Zhao J, Guo X, Feng Y, Zhang B and Tian L. LncRNA MT1JP plays a protective role in intrahepatic cholangiocarcinoma by regulating miR-18a-5p/FBP1 axis. BMC Cancer 2021; 21: 142.

[33] Sharma B, Randhawa V, Vaiphei K, Gupta V, Dahiya D and Agnihotri N. Expression of miR-18a-5p, miR-144-3p, and miR-663b in colorectal cancer and their association with cholesterol homeostasis. J Steroid Biochem Mol Biol 2021; 208: 105822.

[34] Zhang Y and Chen X. miR-18a-5p promotes proliferation and migration of vascular smooth muscle cells by activating the akt/extracellular regulated protein kinases (ERK) signaling pathway. Med Sci Monit 2020; 26: e924625.
[35] Guan JT, Li XX, Peng DW, Zhang WM, Qu J, Lu F, D'Amato RJ and Chi ZL. MicroRNA-18a-5p administration suppresses retinal neovascularization by targeting FGF1 and HIF1A. Front Pharmacol 2020; 11: 276.
[36] Rogg EM, Abplanalp WT, Bischof C, John D, Schulz MH, Krishnan J, Fischer A, Poluzzi C, Schaefer L, Bonauer A, Zeiher AM and Dimmeler S. Analysis of cell type-specific effects of MicroRNA-92a provides novel insights into target regulation and mechanism of action. Circulation 2018; 138: 2545-2558.
[37] Qi C, Lei L, Hu J, Wang G, Liu J and Ou S. Thrombospondin-1 is a prognostic biomarker and is correlated with tumor immune microenvironment in glioblastoma. Oncol Lett 2021; 21: 22.
[38] Adams JC. Thrombospondins: multifunctional regulators of cell interactions. Annu Rev Cell Dev Biol 2001; 17: 25-51.
[39] Sun S, Dong H, Yan T, Li J, Liu B, Shao P, Li J and Liang C. Role of TSP-1 as prognostic marker in various cancers: a systematic review and meta-analysis. BMC Med Genet 2020; 21: 139.
[40] Roberts DD. Thrombospondins: from structure to therapeutics. Cell Mol Life Sci 2008; 65: 669-671.
[41] Mutant p53 aids cancer cells in evading lethal innate immune responses. Cancer Discov 2021; 11: OF14.
[42] Zhao J, Blayney A, Liu X, Gandy L, Jin W, Yan L, Ha JH, Canning AJ, Connelly M, Yang C, Liu X, Xiao Y, Cosgrove MS, Solmaz SR, Zhang Y, Ban D, Chen J, Loh SN and Wang C. EGCG binds intrinsically disordered N-terminal domain of p53 and disrupts p53-MDM2 interaction. Nat Commun 2021; 12: 986.
[43] Muller I, Strozyk E, Schindler S, Beissert S, Oo HZ, Sauter T, Lucarelli P, Raeth S, Hausser A, Al Nakouzi N, Fazli L, Gleave ME, Liu H, Simon HU, Walczak H, Green DR, Bartek J, Daugaard M and Kulms D. Cancer cells employ nuclear caspase-8 to overcome the p53-dependent G2/M checkpoint through cleavage of USP28. Mol Cell 2020; 77: 970-984, e977.
[44] Bykov VJN, Eriksson SE, Bianchi J and Wiman KG. Targeting mutant p53 for efficient cancer therapy. Nat Rev Cancer 2018; 18: 89-102.
[45] Pfaff MJ, Mukhopadhyay S, Hoofnagle M, Chabasse C and Sarkar R. Tumor suppressor protein p53 negatively regulates ischemia-induced angiogenesis and arteriogenesis. J Vasc Surg 2018; 68: 222S-233S, e221.
[46] Linderholm B, Karlsson E, Klaar S, Lindahl T, Borg AL, Elmberger G and Bergh J. Thrombospondin-1 expression in relation to p53 status and VEGF expression in human breast cancers. Eur J Cancer 2004; 40: 2417-2423.
[47] Sundaram P, Hultine S, Smith LM, Dews M, Fox JL, Biyashev D, Schelter JM, Huang Q, Cleary MA, Volpert OV and Thomas-Tikhonenko A. p53-responsive miR-194 inhibits thrombospondin-1 and promotes angiogenesis in colon cancers. Cancer Res 2011; 71: 7490-7501.
[48] Han Y, Jiang Q, Wang Y, Li W, Geng M, Han Z and Chen X. The anti-proliferative effects of oleanolic acid on A7r5 cells-role of UCP2 and downstream FGF-2/p53/TSP-1. Cell Biol Int 2017; 41: 1296-1306.

Supplementary File 1

Supplementary methods

RNA extraction and quantitative real-time polymerase chain reaction (qRT-PCR)

Hemolysis of serum specimens was tested to remove potential contaminants. We routinely assessed the degree of overall RNA integrity to analyze RNA quality. Samples exhibiting an RNA integrity number (RIN) value greater than 7 as determined on an Agilent 2100 Bioanalyzer were included in the analysis. miRNA was isolated from serum samples with a miRNeasy Mini Kit (Qiagen). A total of 500 µl of serum was used for each experiment. For the detection of miR-18a-5p in serum samples, a synthetic C. elegans miRNA (cel-miRNA-39) was used as an internal control due to the lack of universal endogenous controls. miR-18a-5p primers were obtained from Takara Bio (sequences protected by a patent). Other primers were obtained from Sangon Biotech, and detailed primer sequence information is listed in Supplementary Table 1.

Enriched small RNAs from serum were reverse transcribed with a TaqMan MicroRNA Reverse Transcription Kit (Applied Biosystems). The expression of selected miRNAs, cel-miR-39 (for normalization of serum) and U6 (for normalization of cultured cells) was tested with a TaqMan miRNA assay (Applied Biosystems).

Total RNA from cells was extracted using TRIzol reagent (Invitrogen, USA). The RNA concentration and integrity were determined by spectrophotometry and standard RNA gel electrophoresis, respectively. RNA was reverse transcribed into cDNA using a Primer-Script One-Step RT-PCR kit (TaKaRa, Dalian, China). The cDNA template was amplified by real-time PCR using a SYBR Premix DimerEraser kit (TaKaRa). Real-time PCR was performed using specific primers (Supplementary Table 1) for GAPDH, TSP1, IGF1, LIF, CCND2, NACC1 and MMP1 obtaining from Sangon Biotech. CTGF primers were obtained from Takara Bio (sequences protected by a patent). The mean cycle threshold (CT) value for each sample was analyzed using the $2^{-\Delta\Delta CT}$ method. All the reactions were performed in triplicate.

Cell proliferation assay

Cell viability was measured using the Cell Counting Kit-8 (CCK-8) assay (Dojindo Laboratories, Kumamoto, Japan). After transfection for 48 hours, HUVECs were seeded into 96-well plates at a density of 1×10^3 cells per well in 100 µl of medium. Subsequently, 10 µl of CCK-8 solution with 90 µl medium was added to each well at the indicated time points. After incubation at 37°C for 90 min, the absorbance at 450 nm was measured with a plate reader. The growth curves were examined to determine the growth rates.

Transwell assay

HUVECs were seeded into the upper chamber of Transwell® cell culture inserts with an 8 µm pore size (Costar-Corning, USA) in serum-free medium. The lower chamber was filled with MEM-α supplemented with 10% FBS. After an incubation period of 48 h, the cells on the upper surface of the membrane were removed with a cotton swab, while cells in the bottom of the chamber were fixed with 70% ethanol and stained with 0.5% crystal violet solution for 30 min at room temperature. A light microscope was used to count the number of migrated cells (4 random fields per chamber).

Wound healing assay

HUVECs were plated in 6-well plates at a density of 2×10^6 cells per well. After 24 h, wounds were generated using sterilized pipette tips, and the medium was substituted with serum-free medium. Images of the plates in the same field of view were observed and captured 48 h later.

In vitro tube formation assay

In vitro tube formation assays were performed in 96-well plates coated with 50 μl of Matrigel Basement Membrane Matrix, Growth Factor Reduced (Corning, 354230), which was heated at 37°C for 30 min to allow gel formation. Then, 2×10^4 HUVECs subjected to various transfections in MEM-α containing 2% FBS were seeded onto the Matrigel and incubated at 37°C for 8 h. The formation of tubes and tube-like structures was captured 8 h later using a Nikon Eclipse 80i microscope (Nikon, Japan).

RNA immunoprecipitation (RIP)

HUVECs (2×10^6) were seeded onto 10 cm tissue culture plates and transfected with 4 μg of FLAG-AGO2 and 25 nM scr/mimic miR-18a-5p using Lipofectamine 2000 (Life). HUVECs were transfected with pBSKS (an empty plasmid) as a negative control. After transfection for 48 hours, cells were washed with ice-cold 1× PBS, scraped, and transferred to a 1.5 ml tube, followed by centrifugation at 200×g for 2 min. The cells were then resuspended in 200 μl of cold resuspension buffer (20 mM Tris (pH = 7.5), 150 mM NaCl, 1 mM EDTA, 1 mM EGTA) containing 1 U/μl RNasin Plus (Promega) and lysed by the addition of 800 μl of cold lysis buffer (1% Triton X-100, 20 mM Tris (pH = 7.5), 150 mM NaCl, 1 mM EDTA, 1 mM EGTA, 1 mM phenylmethyl-sulfonyl fluoride (PMSF, Sigma), 1X complete EDTA-free Protease Inhibitor cocktail (Roche) and incubation on ice for 10-30 min. After centrifugation (10,000×g for 10 min at 4°C), 10 μl of RQ1 DNase (Promega) was added to the supernatant. IP of FLAG-AGO2 was performed with anti-FLAG M2 mouse antibody (Sigma, F3165) for 3 h at 4°C with rotation. After undergoing five washes with lysis buffer, 10% of the sample beads were subjected to protein extraction and WB by adding LDS sample buffer and DTT and heating the samples at 70°C for 20 min. The remaining 90% of the sample beads were incubated with RQ1 DNase for 30 min for later RNA extraction with TRIzol (Invitrogen, USA).

Establishment of an animal model of VM

Six-week-old athymic BALB/c nu/nu male mice (purchased from ProMedican Pharmaceutical Co.) were used to establish the VM model. HUVECs (5×10^6) stable cell lines which expressing TIE2 protein (WT or L914F mutation) were subcutaneously inoculated into either side of the flank area in an equivalent volume of Matrigel (n = 3 for each group). The lesions were harvested 2 weeks after inoculation and subjected to HE staining. For the miR-18a-5p treatment experiment, HUVECs with the TIE2-L914F mutation were transfected with miR-18a-5p mimic, inhibitor or vehicle for 72 h before subcutaneous injection into mice as previously described (n = 6 per group). The lesion area was measured with Vernier calipers every 3 days, and the final lesions were harvested at 18 days after inoculation. The weight of lesions and the vessel structures were observed after HE staining. All animal experiments were performed in the animal laboratory center of the Ninth People's Hospital, Shanghai Jiaotong University School of Medicine (Shanghai, China), and were conducted in accordance with the Guide for the Care and Use of Laboratory Animals published by the US National Institutes of Health (NIH publication number 85-23, revised 1996). The study protocol was approved by the Animal Care and Use Committee of the Ninth People's Hospital (SH9H-2019-A486-1).

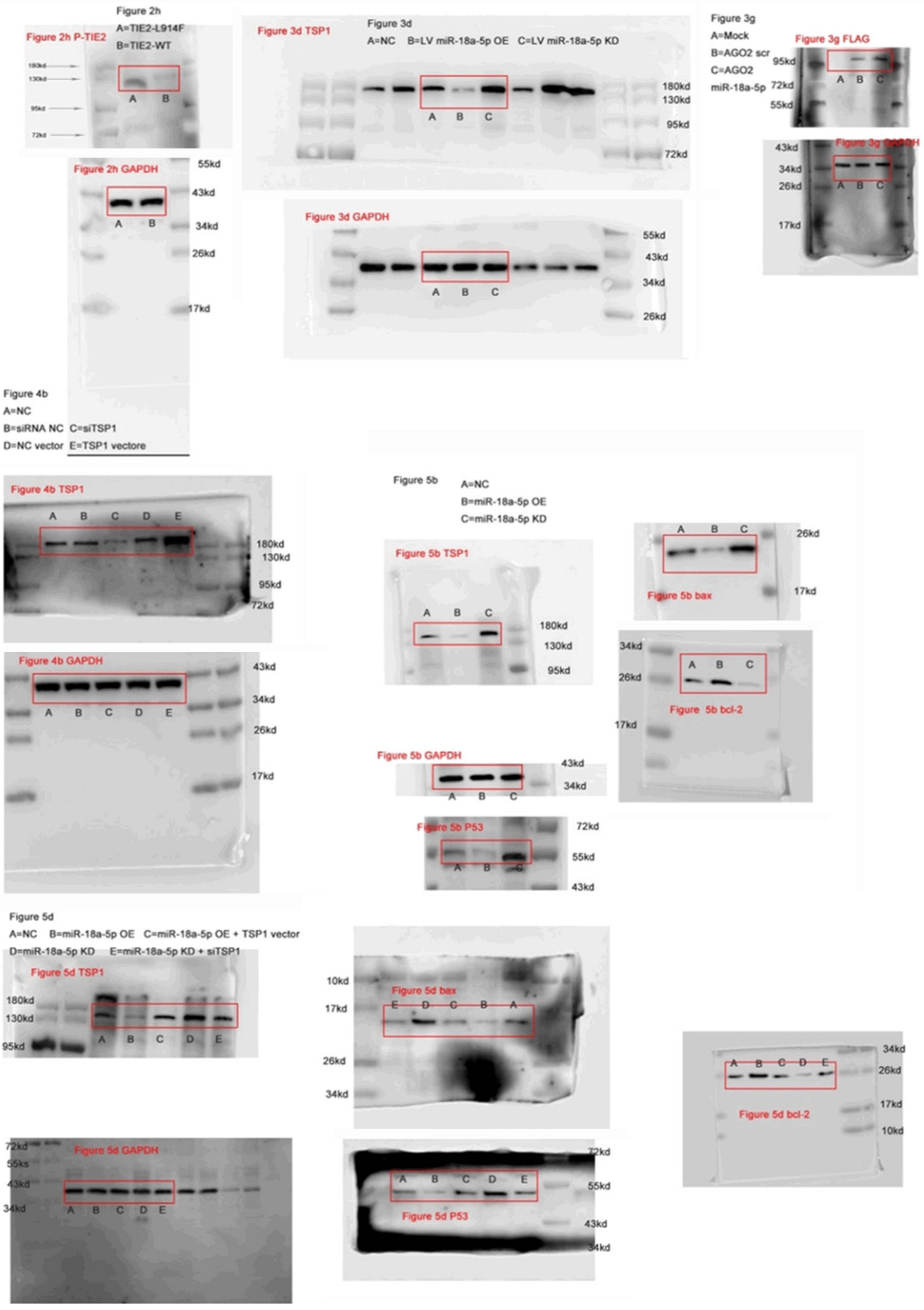

Supplementary Figure 1. Original, full-length gel and blot images.

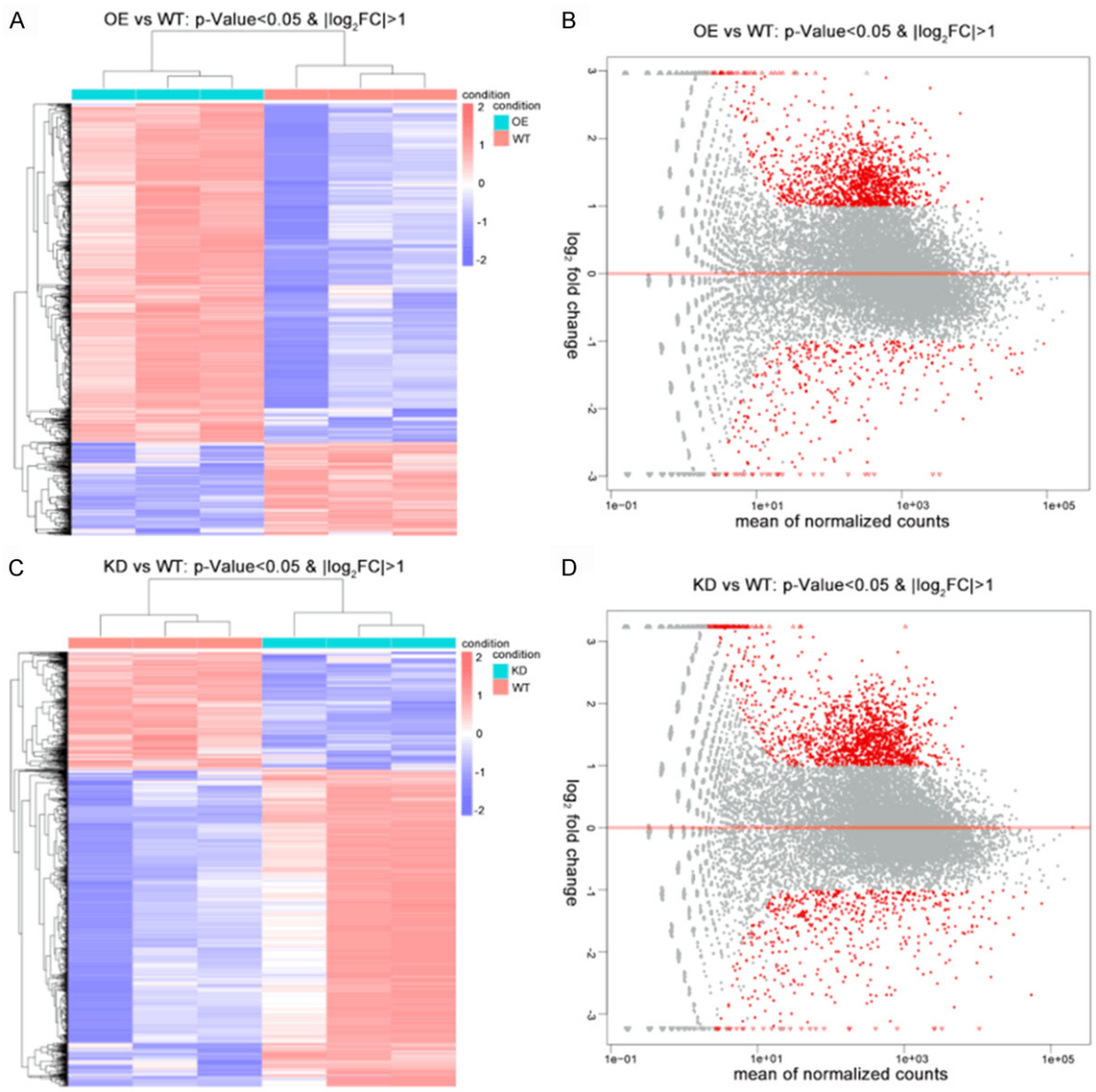

Supplementary Figure 2. A, C. A heatmap showing the genes differentially expressed between the miR-18-5p changed group and the control group as indicated via RNA-seq is shown. B, D. Volcano plot showing all differentially expressed genes between the miR-18-5p changed group and the control group as indicated via RNA-seq is shown.

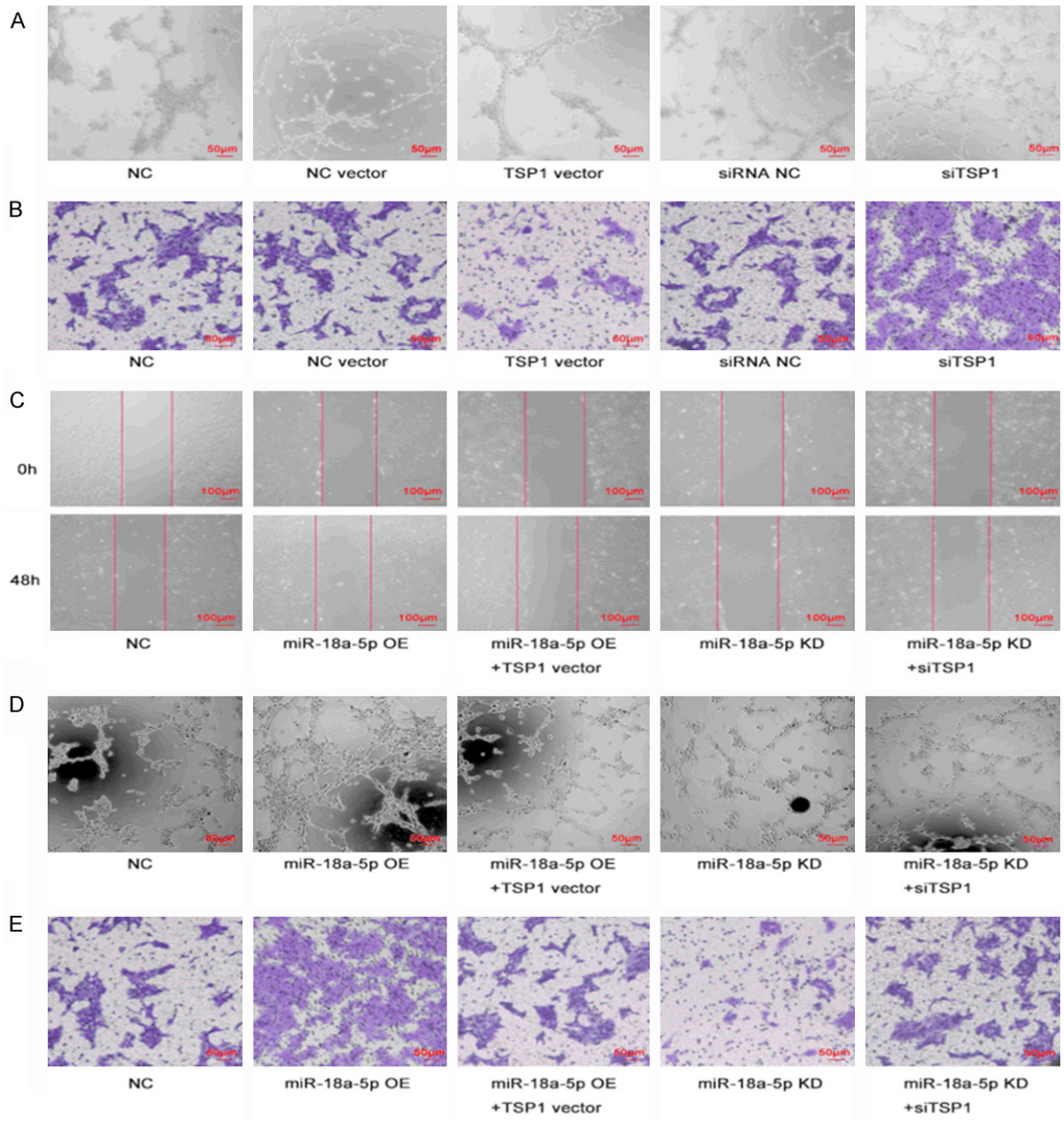

Supplementary Figure 3. (A, B) Angiogenesis and migration of HUVECs transfected with NC, NC vector, TSP1 vector, siRNA NC or siTSP1 were evaluated by tube formation (A) and transwell assays (B), respectively. (C-E) Invasion, angiogenesis and migration of HUVECs transfected with NC, miR-18a-5p OE, miR-18a-5p OE + TSP1 vector, miR-18a-5p KD and miR-18a-5p KD + siTSP1 were evaluated by wound healing (C), tube formation (D) and transwell assays (E), respectively.

A

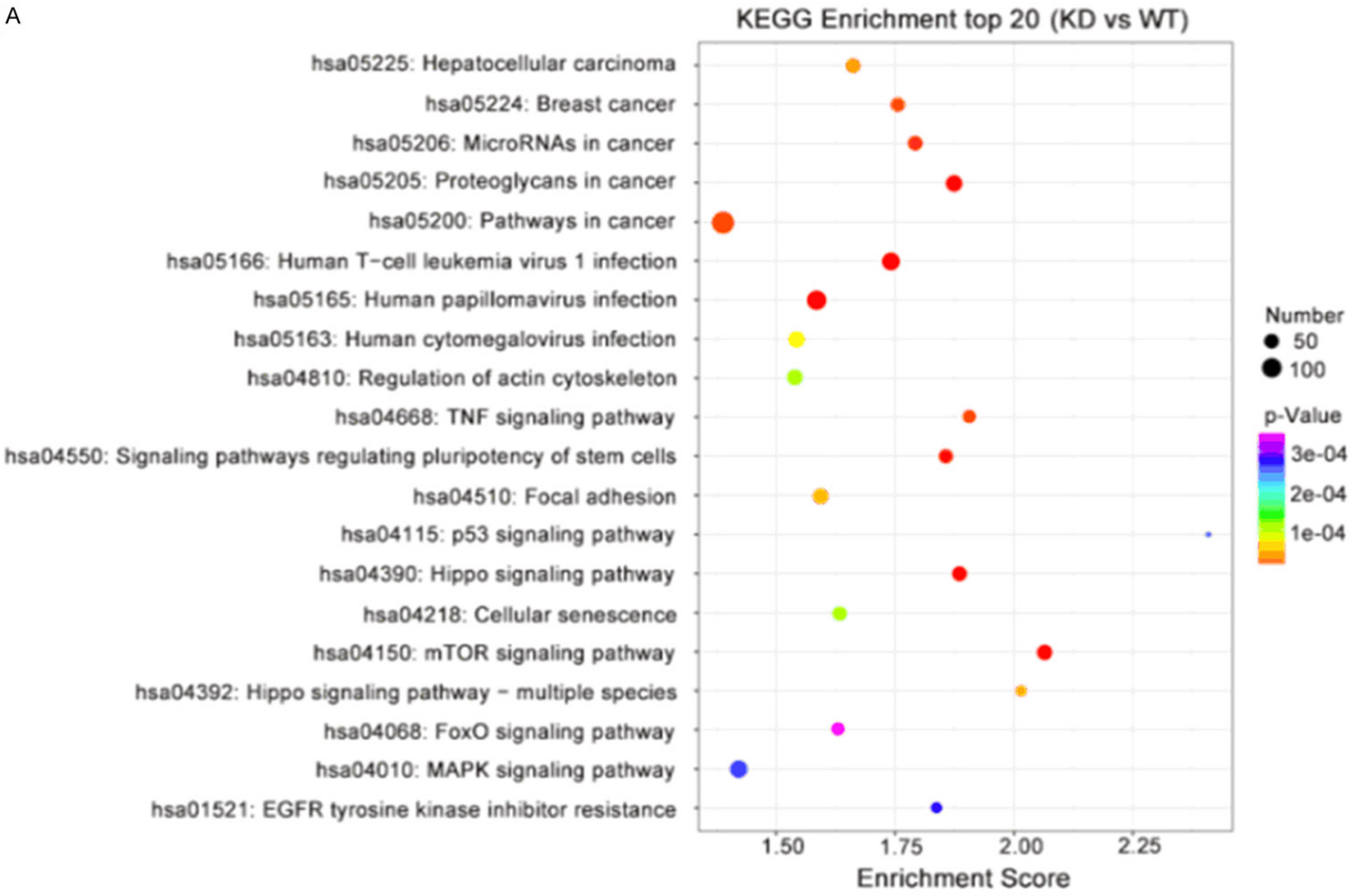
KEGG Enrichment top 20 (KD vs WT)
hsa05225: Hepatocellular carcinoma
hsa05224: Breast cancer
hsa05206: MicroRNAs in cancer
hsa05205: Proteoglycans in cancer
hsa05200: Pathways in cancer
hsa05166: Human T−cell leukemia virus 1 infection
hsa05165: Human papillomavirus infection
hsa05163: Human cytomegalovirus infection
hsa04810: Regulation of actin cytoskeleton
hsa04668: TNF signaling pathway
hsa04550: Signaling pathways regulating pluripotency of stem cells
hsa04510: Focal adhesion
hsa04115: p53 signaling pathway
hsa04390: Hippo signaling pathway
hsa04218: Cellular senescence
hsa04150: mTOR signaling pathway
hsa04392: Hippo signaling pathway − multiple species
hsa04068: FoxO signaling pathway
hsa04010: MAPK signaling pathway
hsa01521: EGFR tyrosine kinase inhibitor resistance
1.50
1.75
2.00
2.25
Enrichment Score
Number
50
100
p-Value
3e-04
2e-04
1e-04

B

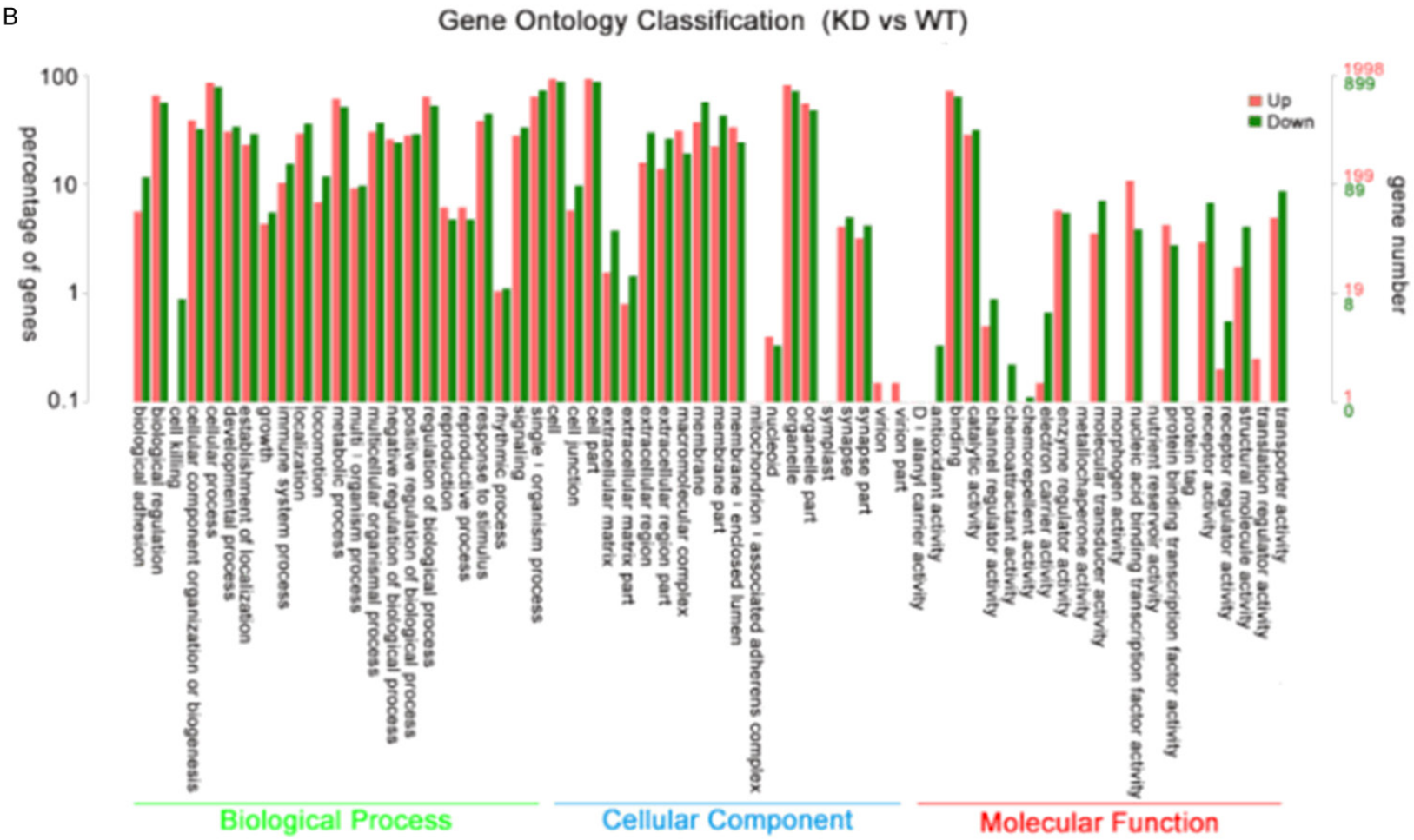
Gene Ontology Classification (KD vs WT)
percentage of genes
100
10
1
0.1
gene number
1998
899
199
89
19
8
1
0
Up
Down
biological adhesion
biological regulation
cell killing
cellular component organization or biogenesis
cellular process
developmental process
establishment of localization
growth
immune system process
localization
locomotion
metabolic process
multi-organism process
multicellular organismal process
negative regulation of biological process
positive regulation of biological process
regulation of biological process
reproduction
reproductive process
response to stimulus
rhythmic process
signaling
single-organism process
cell
cell junction
cell part
extracellular matrix
extracellular matrix part
extracellular region
extracellular region part
macromolecular complex
membrane
membrane part
membrane-enclosed lumen
mitochondrion-associated adherens complex
nucleoid
organelle
organelle part
symplast
synapse
synapse part
virion
virion part
D-alanyl carrier activity
antioxidant activity
binding
catalytic activity
channel regulator activity
chemoattractant activity
chemorepellent activity
electron carrier activity
enzyme regulator activity
metallochaperone activity
molecular transducer activity
morphogen activity
nucleic acid binding transcription factor activity
nutrient reservoir activity
protein binding transcription factor activity
protein tag
receptor activity
receptor regulator activity
structural molecule activity
translation regulator activity
transporter activity
Biological Process
Cellular Component
Molecular Function

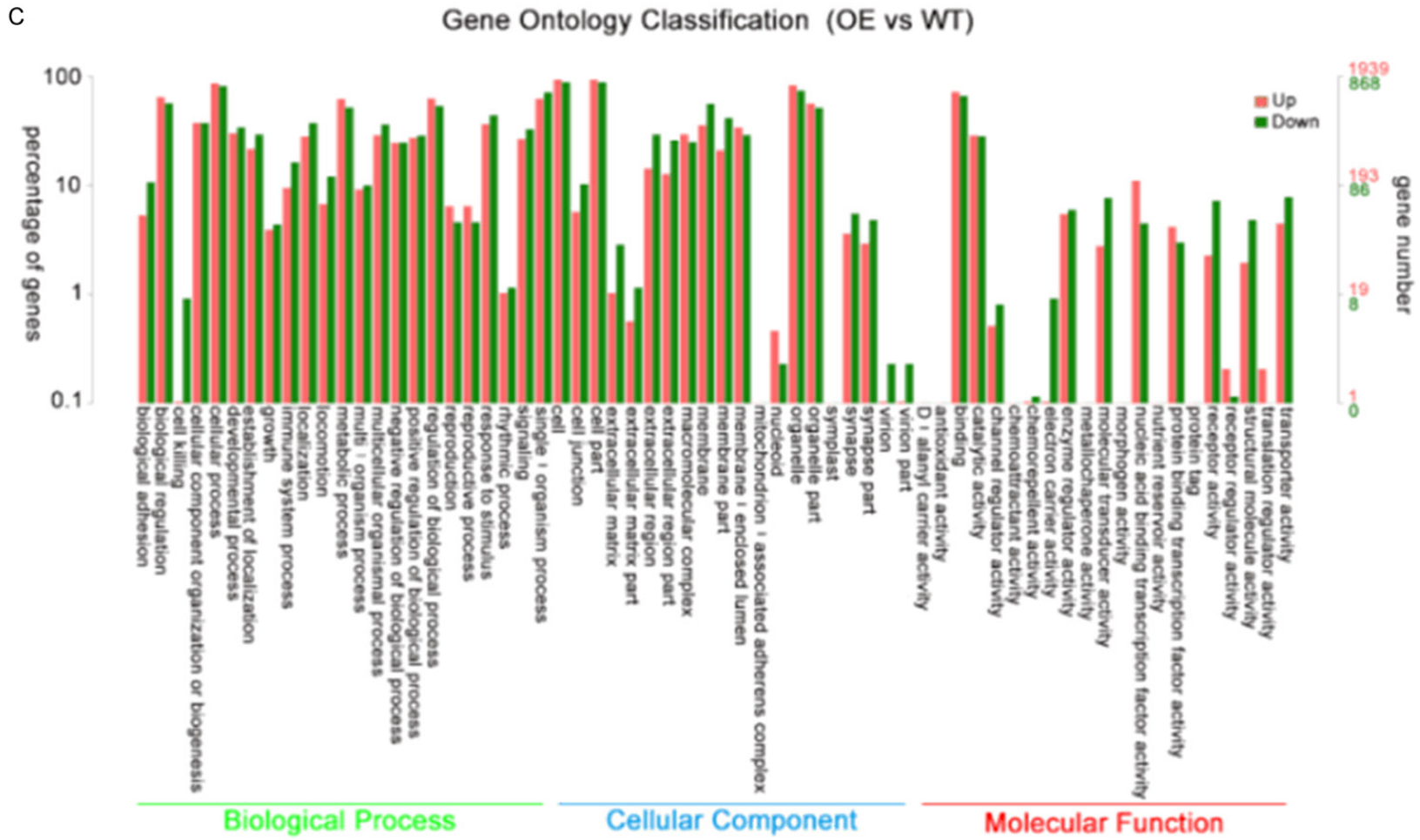

Supplementary Figure 4. (A) KEGG analysis was used to identify pathway terms enriched in the dysregulated mRNAs in HUVECs with miR-18a-5p KD vs WT. (B, C) GO term enrichment analysis of the biological process (BP), cellular component (CC) and molecular function (MF) categories for the dysregulated mRNAs (B: KD vs WT, C: OE vs WT).

Supplementary Table 1. Primers of genes used for this study

Primer	Sequences
Cel-miR-39	Forward Primer 5'-CAGAGTCACCG GGTGTAAAT-3'
	Reverse Primer 5'-CCAGTGC GTGTCGTGGAGTC-3'
U6	Forward Primer 5'-CTCGCTTCGGCAGCACATATACT-3'
	Reverse Primer 5'-ATTTGCGTGTCATCCTTGCGCA-3'
TSP-1	Forward Primer 5'- GCCATCCGCACTAACTACATT-3'
	Reverse Primer 5'-TCCGTTGTGATAGCATAGGGG-3'
IGF1	Forward Primer 5'-GCTCTTCAGTTCGTGTGTGGA-3'
	Reverse Primer 5'-GCCTCCTTAGATCACAGCTCC-3'
NACC1	Forward Primer 5'-CTCTCCCGGCTGAACTTATCA-3'
	Reverse Primer 5'-AGCGTGTTCCGGTCAAAGAA-3'
LIF	Forward Primer 5'-GCATCAACTCCGCAGCTTAG-3'
	Reverse Primer 5'-CTGAACGCCATAGCCAGGTCT-3'
CCND2	Forward Primer 5'-ACCTTCCGCAGTGCTCCTA-3'
	Reverse Primer 5'-CCCAGCCAAGAAACGGTCC-3'
MMP1	Forward Primer 5'-AAAATTACACGCCAGATTTGCC-3'
	Reverse Primer 5'-GGTGTGACATTACTCCAGAGTTG-3'
GAPDH	Forward Primer 5'- GGAGCGAGATCCCTCCAAAAT-3'
	Reverse Primer 5'- GGCTGTTGTCATACTTCTCATGG-3'